Title: Transposon mutagenesis screen in *Klebsiella pneumoniae* identifies genetic determinants required for growth in human urine and serum

Jessica Gray[1,2#], Von Vergel L Torres[1#], Emily CA Goodall[1], Karl A Dunne[2], Chris Icke[1], Jessica L Rooke[1], Thamarai Schneiders[3], Adam F Cunningham[4], Jeffrey A Cole[2], Ian R Henderson[1*]

1. Institute for Molecular Bioscience, University of Queensland, St. Lucia, Queensland, Australia
2. Institute of Microbiology and Infection, University of Birmingham, Birmingham, United Kingdom
3. Division of Infection Medicine, University of Edinburgh, Edinburgh, United Kingdom
4. Institute of Immunology and Immunotherapy, University of Birmingham, Birmingham, United Kingdom

# Authors contributed equally
*For correspondence: i.henderson@uq.edu.au

Abstract

Klebsiella pneumoniae is a global public health concern due to the rising myriad of hypervirulent and multi-drug resistant clones both alarmingly associated with high mortality. The molecular microbial genetics underpinning these recalcitrant *K. pneumoniae* infections is unclear, coupled with the emergence of lineages resistant to nearly all present day clinically important antimicrobials. In this study, we performed a genome-wide screen in *K. pneumoniae* ECL8, a member of the endemic K2-ST375 pathotype most often reported in Asia, to define genes essential for growth in a nutrient-rich laboratory medium (Luria-Bertani medium), human urine and serum. Through transposon directed insertion-site sequencing (TraDIS), a total of 427 genes were identified as essential for growth on LB agar, whereas transposon insertions in 11 and 144 genes decreased fitness for growth in either urine or serum, respectively. Genome-wide functional studies like these provide further knowledge on the genetics of this pathogen but also provide a strong impetus for discovering new antimicrobial targets to improve current therapeutic options for *K. pneumoniae* infections.

Introduction

Klebsiella pneumoniae are Gram-negative bacteria found ubiquitously in natural and man-made environments [1-3]. In immunocompromised patients, and those with co-morbidities such as diabetes or alcoholism, *K. pneumoniae* can colonize multiple body sites causing a diverse array of infections ranging from life-threatening pneumonia, urinary tract infections (UTIs), and bacteremia [4-8]. *K. pneumoniae* is a frequently reported multidrug-resistant (MDR) pathogen isolated from nosocomial settings. Such infections have generally higher mortality rates and require longer treatment regimens and hospital stays, placing a significant burden on healthcare providers [9-11]. Of most concern is resistance to β-lactam antibiotics such as penicillin, aztreonam, and extended-spectrum cephalosporins, by horizontally acquired plasmid-mediated β-lactamases [12]. While combined antibiotic therapies have been deployed in the clinic, the emergence of pandrug-resistant strains has created an urgency to develop new and efficient approaches to treating *K. pneumoniae* infections [13-15]. The identification of genetic determinants essential for growth and those required for survival of *K. pneumoniae in vivo* may help elucidate novel therapeutic targets to better treat such infections [16, 17].

Recent large scale phylogenetic investigations have suggested that distinct lineages of *K. pneumoniae* exist in clinical and environmental settings [18]. Furthermore, two clinical pathotypes of *K. pneumoniae* have emerged: classical and hypervirulent. While the full repertoire of genetic factors required for *K. pneumoniae* virulence remains unclear, various studies have highlighted the importance of genes involved in adhesion, iron acquisition, capsulation and cell envelope biogenesis [19]. Nevertheless, for both classical and hypervirulent *K. pneumoniae* strains, the ability to colonize the urinary tract and survive in

the bloodstream are essential virulence traits and are dependent on a large and diverse range of virulence factors [20]. Indeed, previous studies demonstrated that lipopolysaccharide (O-) (9 serotypes) and capsular polysaccharide (K-) antigens (79 serotypes) contribute to the resistance of serum-mediated killing and antiphagocytosis [21, 22]. However, prior genetic screens have revealed that serum-resistance in Gram-negative bacteria is an intricate phenotype defined by a multitude of factors (the serum resistome) [23-27]. A recent study of *K. pneumoniae* identified 93 different genes associated with serum resistance across four distinct strains but found only three genes (*lpp*, *arnD*, and *rfaH*) played a role in all strains. These data hint that multiple mechanisms of serum resistance may exist in *Klebsiella* lineages. In contrast, the full repertoire of genes required for growth of *K. pneumoniae* in the urinary tract (the urinome) has not been defined.

To define the genetic basis of the *K. pneumoniae* urinome and serum resistome, we used Transposon Insertion Sequencing (TIS), also referred to as Transposon Directed Insertion-site Sequencing (TraDIS). TraDIS is a genome-wide screening technique that has been widely used to identify genes essential for bacterial growth and to discover conditionally essential genes under physiologically relevant conditions [28-38]. In this study, we generated a highly saturated transposon library within *K. pneumoniae* ECL8, a member of the K2-ST375 phylogenetic lineage that includes hypervirulent clones of epidemiological significance known to cause infections in relatively healthy subjects predominantly in Asia [39]. We identified the repertoire of genes essential for growth in laboratory conditions, in pooled human urine, and in human serum. Selected fitness-genes were validated for growth in pooled urine or serum by generating single-gene deletion mutants. Our study provides insight into the molecular mechanisms that enable *K. pneumoniae* to survive *in vivo* and cause disease.

Methods

Bacterial strains, plasmids, and culturing conditions.

A complete list of bacterial strains, plasmids, and primers utilized in this study are listed in Table S1 and Table S2. To culture strains, scrapings from a frozen glycerol stock strain were plated onto solid Luria-Bertani (LB) (10 g tryptone, 5 g yeast extract, 10 g NaCl) supplemented with agar 1.5% (w/v) and were incubated overnight at 37°C. A single colony was isolated and used to inoculate 5 mL of liquid LB medium incubated overnight at 37°C with 180 RPM shaking. To prepare stocks, bacteria were grown to mid-exponential phase in LB medium and stored at -80°C with 25% (v/v) glycerol. When required, solid or liquid media were supplemented with appropriate antibiotics at the following concentrations: ampicillin (35 µg/mL); chloramphenicol (100 µg/mL); and kanamycin (100 µg/mL).

Generation of the *K. pneumoniae* ECL8 transposon mutant library

An overnight culture of *K. pneumoniae* ECL8 was inoculated into 2× YT broth at OD_{600} 0.05 supplemented with a final concentration of 0.7 mM EDTA and incubated at 37°C with 180 RPM shaking. Cells were harvested at 0.4 OD_{600} by centrifugation (4,000 *g*) at 4°C for 20 min. Cell pellets were washed 4 times with ice-cold 10% (v/v) glycerol. *K. pneumoniae* ECL8 electrocompetent cells were transformed with 0.2 µL of EZ-Tn*5*™ transposon (Epicentre) at 1.4 kV and recovered in brain heart infusion (BHI) broth for 2 h at 37°C with 180 RPM shaking. Cells were plated onto LB agar supplemented with 50 µg/mL kanamycin and incubated overnight at 37°C. More than 1 million transformants were pooled in 15% (v/v) LB-glycerol for storage at -80°C until required.

Transposon library screening in human urine

Human urine from 7 healthy male volunteers was sterilized using a vacuum filter (0.2 µM). Urine was pooled and stored at -80℃ until required. Approximately 2 × 10^8 *K. pneumoniae* ECL8 TraDIS mutants were inoculated into 50 mL of urine and grown for 12 h at 37℃ with shaking (P1) in biological duplicates in parallel with control samples that were instead inoculated into 50 mL of LB medium. A sample of P1 was inoculated into 50 mL of urine or LB medium, respectively, at an initial OD_{600} of 0.05 and grown for a subsequent 12 h (P2). Both control and test experiments were passaged and grown for a further 12 h (P3). A sample of culture from P3 was removed and normalized to an OD_{600} of 1 for subsequent genomic DNA extraction.

Transposon library screening in human serum

A 10 mL sample of human blood was collected from 8 healthy volunteers. Blood was pooled and centrifuged at 6,000 *g* for 20 min to separate sera from blood components. The pooled serum was sterilized, aliquoted and stored at -80℃ until required. Approximately 2 x 10^8 *K. pneumoniae* ECL8 mutants were inoculated into 1 mL of pre-warmed sera, heat-inactivated sera (60℃ for 1 h) or PBS in biological duplicates. Samples were incubated at 37°C for 90 min with 180 RPM shaking. Following this, cells were harvested by centrifugation at 6,000 *g* for 10 min and washed twice with PBS. Cells were then inoculated into 50 mL of LB for outgrowth at 37℃ with 180 RPM shaking and harvested at an OD_{600} of 1 by centrifugation at 6,000 *g* for 10 min. A 1 mL sample of each culture was used for genomic DNA extraction.

Transposon library sequencing and data analysis.

127 Pooled kanamycin resistant *K. pneumoniae* ECL8 cells were prepared for sequencing following
128 an amended TraDIS protocol [28](21). Briefly, genomic DNA from the *K. pneumoniae* ECL8
129 library of pooled mutants was extracted from ~1×10^9 cells in biological duplicate, as per
130 manufacturer's instructions (Qiagen QIAamp DNA blood minikit). The DNA concentration of
131 replicates was determined using the Qubit 2.0 fluorometer (Thermo Fisher Scientific). The
132 DNA was sheared into ~200 bp fragments by ultra-sonication (Bioruptor Plus Diagenode).
133 Fragmented DNA samples were prepared for Illumina sequencing using the NEBNext Ultra I
134 DNA Library Prep Kit for Illumina according to manufacturer's instructions with the following
135 modifications: ends of fragmented DNA were repaired using the End Prep Enzyme Mix (NEB)
136 and an NEBNext adaptor for Illumina sequencing was ligated to the newly repaired ends.
137 During protocol optimization, samples were analyzed using a Tapestation 2200 (High
138 Sensitivity D5000) to determine DNA fragment sizes following adapter ligation. The uracil
139 within the adaptor hairpin loop was enzymically excised using the USER enzyme (NEB).
140 AMPure XP SPRI beads (Beckman Coulter) or custom-made SPRI beads were used to select
141 for DNA fragments ~250 bp in size.
142
143 To enrich for fragments containing the transposon a custom PCR step was introduced using a
144 forward primer annealing to the 3' end of the antibiotic marker of the transposon and a
145 reverse primer that annealed to the ligated adaptor. The PCR product was purified using SPRI
146 beads at a ratio of 0.9:1 (beads:sample). A further custom PCR step introduced sequencing
147 flow-cell adaptors (Illumina barcodes) and inline barcodes to allow for sample multiplexing
148 (Table S3). Samples were then stored at -20°C until sequencing. After qRT-PCR (KAPA Library
149 Quantification Kit Illumina® Platforms) to determine TraDIS library concentration, a 1.5 µL
150 sample of each library sample diluted to 8 nM was combined and mixed by pipetting to

generate a pooled amplified library (PAL) of samples for multiplexed sequencing. The PAL was prepared for Illumina MiSeq sequencing according to manufacturer's instructions.

Bioinformatic analysis of sequencing reads was completed on the Cloud Infrastructure for Microbial Bioinformatics (CLIMB) [40]. Raw fastQ files were first demultiplexed according to Illumina barcodes automatically using the Illumina MiSeq software.Experimental replicates were separated by custom inline barcodes using the FastX barcode splitter and the barcodes were subsequently removed using the FastX trimmer (v0.0.13). Each read was checked for the presence of the transposon sequence in two steps; first, reads that contained the first 25 bp of the transposon sequence (AGCTTCAGGGTTGAGATGTGTA), introduced by the TKK_F primer, allowing for 3 mismatches were filtered and parsed. Parsed reads were subsequently checked for the presence of the final 10 bp of the transposon sequence (TAAGAGACAG), allowing for 1 mismatch. The transposon sequence and reads <20 bp were trimmed using Trimmomatic (v0.39). Resulting reads were mapped to the *K. pneumoniae* ECL8 [HF536482.1 and HF536483] genome and plasmid using the Burrows-Wheeler Alignment tool (BWA-MEM). Mapped reads were indexed using samtools (v1.8) and converted into bed format using the Bam2bed tool (Bedtools suite v2.27.1). The resulting bed file was intersected against the annotated CDS in the *K. pneumoniae* ECL8 gff file, which was generated using PROKKA (v1.14.0). Transposon insertion sites and their corresponding location were quantified using custom python scripts. Mapped transposon insertion sites were visualized using the Artemis genome browser [41].

Statistical analysis of transposon insertion density

A modified geometric model was applied to identify the probability of finding k-1 insertion-free bases followed by a transposon insertion as reported previously [28](21). In a string of 10,000 independent trials the probability of an insertion 'p' was calculated using the following equation: P(k) = p(1-p)(k).

Identification of putative essential genes

In-house scripts kindly provided by Langridge and colleagues [42](34) were amended and used for the prediction of essential genes. Briefly, the number of unique transposon insertion sites for each gene was normalized for CDS length (number of UIPs/CDS length in bp), which was denoted the insertion index score. The Freedman-Diaconis method was used to generate a histogram of the insertion index scores for each gene of the *K. pneumoniae* ECL8 TraDIS library. Distributions were fitted to the histogram using the R MASS library (v4.0.0).

An exponential distribution was applied to the 'essential' mode, situated on the left of the histogram. A gamma distribution was applied to the 'non-essential' mode, situated on the right of the histogram. The probability of a gene belonging to each mode was calculated and the ratio of these values was denoted the log-likelihood score. Genes were classified as 'essential' if they were 12 times more likely to be situated in the left mode than the right mode. Genes with log-likelihood scores between the upper and lower $\log_2(12)$ threshold values of 3.6 and -3.6 respectively were classified as 'unclear'. Genes with log-likelihood scores below the 12-fold threshold were classified as 'non-essential'.

Comparison of essential gene lists between ECL8, KPNIH1, RH201207 and ATC43816

Annotated genomes of *K. pneumoniae* KPNIH1 (Accession: CP009273.1), RH201207 (Accession: FR997879.1), and ATCC 43816 (Accession: CP009208.1) were downloaded from NCBI. Nucleotide sequences of putative essential genes were extracted using the SeqKit toolbox [43](33). *K. pneumoniae* ECL8 essential gene homologs were identified in KPNIH1, RH201207 and ATC43816 using Galaxy AU NCBI BLAST+ wrapper blastn using the following criteria (e-value > 1e-10, percent identity >90) and utilizing the top hit based on calculated e value and bitscore [44].

BioTraDIS analysis for the identification of conditionally advantageous genes

To identify conditionally essential genes, we used the Bio-Tradis analysis pipeline [17], that measures the read count $\log_2$ fold changes between each CDS. To ensure robust analysis, CDS with <50 sequence reads in either the test or control condition were filtered and binned. CDS with a $\log_2$ fold-change >2 (test/control) and a Q-value of >0.05 were classified as conferring a fitness advantage under the conditions tested. To comparatively and analyze the impact of transposon insertion-events in genomic regions in the serum-resistant dataset (180 min) to the input, we used the AlbaTraDIS package (v1.0.1) with the following parameters: -a -c 10.0 -f 2 -m 0 [45].

Generation of knock-out strains

Mutants derived from *K. pneumoniae* ECL8 were constructed using the λ Red recombinase system [46]. Briefly, the *K. pneumoniae* ECL8 strain was transformed with pACBSCSE, which contains genes coding for the arabinose-induced λ Red recombinase system that permits homologous recombination between dsDNA PCR products and target loci in the bacterial genome. The recombination is based on short stretches of flanking homology arms (~65bp)

221 with the site of recombination. Using pKD4 as a template for the selectable kanamycin
222 cassette, the PCR products used for replacing the target genes were amplified, gel extracted,
223 and electroporated into electro-competent strain *K. pneumoniae* ECL8 harboring pACBSCSE
224 prepared in the presence of 0.5% (w/v) arabinose. Candidate mutants were screened using
225 antibiotics, verified by PCR using primers outside the region of recombination then followed
226 by SangerSanger sequencing.
227
228 **Bacterial growth assay**
229 A single colony of each bacterial strain was inoculated into 5 mL of LB medium and grown
230 overnight as previously described. Strains were normalized to an OD_{600} of 1.00 and washed
231 twice in PBS by centrifugation at 6,000 *g* for 10 min. Cell pellets were resuspended in 1 mL of
232 the growth medium required for the bacterial growth assay. Greiner Bio-One 96-well U-
233 bottom microtiter plates were inoculated with bacterial strains at an initial OD_{600} of 0.02 in a
234 final well medium volume of 150 µL and sealed with a Breathe-Easy® sealing membrane
235 (Sigma Aldrich). Inoculated plates were incubated at 37°C with 300 RPM shaking, OD_{600}
236 measurements were taken at 15 min over 24 h using a CLARIOstar® plate reader (BMG
237 LABTECH).
238
239 **Urine co-culture competition studies between K. pneumoniae ECL8 and isogenic mutants**
240 Overnight cultures of *K. pneumoniae* ECL8 and an isogenic mutant were normalized to an
241 OD_{600} of 1.00 and washed twice with PBS. Cell pellets were resuspended in 1 mL of urine. A
242 500 µL of either the WT or mutant culture were inoculated into 25 mL of urine and incubated
243 at 37°C with 180 RPM shaking for 12 h. The sample was then transferred to 25 mL of fresh
244 urine at an initial OD_{600} of 0.05 and grown for a further 12 h. The culture was passaged for a

245 further 12 h of growth. These cultures were serially diluted in PBS at 0, 6, 12, 24 and 36 h and
246 plated onto LB agar. Following overnight growth, agar plates were replica plated onto either
247 LB agar or LB agar supplemented with 100 µg/mL kanamycin grown overnight at 37°C then
248 enumerated. Relative fitness was calculated as a competitive index (CI), defined as ratio of
249 mutant:WT viable cells divided by the corresponding inoculum.
250
251 **Lipopolysaccharide extraction**
252 A single colony of ECL8 was inoculated into 5 mL of LB medium and incubated overnight at
253 37°C with 180 RPM shaking. Overnight cultures were normalized to an OD_{600} of 1.00 and
254 centrifuged at 14,000 *g* for 10 min. Cells were resuspended in 100 µL of cracking buffer (0.125
255 M Tris-HCl, 4% (w/v) SDS, 20% (v/v) Glycerol, 10% (v/v) 2-mercaptoethanol in dH2O). The cell
256 suspension was incubated at 100°C for 5 min and transferred to -80°C for 5 min. The cell
257 suspension was incubated at 100°C for a further 5 min and centrifuged at 14,000 *g* for 10 min.
258 An 80 µL sample of the supernatant was transferred to a new tube and incubated with 5 µL
259 of 5 mg/mL Proteinase K (QIAGEN) for 1 h at 60°C. Samples were diluted ×2 with Laemmli
260 sample buffer (Sigma-Aldrich) and incubated at 95°C for 5 min. Samples were loaded onto a
261 4-12% Bis-tris precast NuPAGE gel (Invitrogen) and run at 150 V for 1.5 h. LPS was visualized
262 by silver staining using the SilverQuest kit (Invitrogen) following manufacturer's instructions.
263
264 **Serum bactericidal assay (SBA)**
265 Pooled serum was thawed on ice and pre-warmed to 37°C. Overnight cultures of bacterial
266 strains were normalized to an OD_{600} of 1.00 in LB medium. Bacterial cells were washed twice
267 with PBS and resuspended in a final volume of 1 mL PBS. A 50 µL sample of the cell suspension
268 was inoculated into 50 µL of sera. Sera and cell samples were incubated at 37°C with 180 RPM

shaking. Viable bacterial cells were enumerated by plating 10 µL of cell and sera suspension onto LB agar over a time-course: 0 min, 30 min, 60 min, 90 min, 180 min. Serum bactericidal activity was plotted as the $\log_{10}$ change in colony forming units (CFU) relative to the initial inoculum.

Results and discussion

Generation and sequencing of a *Klebsiella pneumoniae* strain ECL8 transposon input library

A *K. pneumoniae* ECL8 mini-Tn5 mutant library composed of >1 million mutants was constructed and subsequently subjected to TraDIS. The resulting reads were mapped to the reference genome that consists of a ~5.3 Mb chromosome and a single 205-kb plasmid (EMBL Accessions: HF536482.1 and HF536483) (Figure 1A-B). The gene insertion index scores of the two technical replicates of the *K. pneumoniae* ECL8 TraDIS library (KTL1 and KTL2) were highly correlated with each other (R^2=0.955) demonstrating a high level of reproducibility (Figure S1A). Therefore, sequence reads for both replicates were combined for downstream analysis and essential gene prediction. Through iterative rounds of sequencing, we determined that the library was sequenced to near saturation as the discovery of unique reads plateaued at ~2 million reads (Figure S1B). This library contained 554,834 unique genome-wide transposon insertion sites and 499,919 of these insertions map within annotated coding sequence (CDS) boundaries. This high level of transposon coverage equates to an average transposon insertion every 9.93 bp throughout the genome, equivalent to an insertion approximately every four codons. A de Brujin graph visualized in the genome assembly package Bandage [47](38) revealed that the sequencing coverage of the plasmid was only 1.33 fold higher than that of the chromosome indicating that the plasmid is likely present as a single copy (Figure S2). Table 1 summarizes the data relating to the ECL8 libraries.

Table 1: Summary of transposon-containing sequence reads and unique insertion points (UIPs) mapped to the *K. pneumoniae* ECL8

Sample	Mapped reads after QC	Genome-wide UIPs	CDS UIPs	Pearson Correlation of Replicates
ECL8 Input libraries (LB)				
KTL1	5,573,710	409,069	367,230	Figure S1A
KTL2	2,854,389	400,915	361,272	
KTL (Combined)	8,429,782	554,834	499,919	
Urine output libraries				
LB	4,324,125	4,324,125	403,381	Figure S7
Urine	4,839,277	4,839,277	389,251	
Serum output libraries				
Serum	4,729,032	115,328	101,348	Figure S9
Heat-inactivated serum	3,565,433	284,761	254,735	
180 min serum exposed	1,481,732	133,790	121,316	Figure S10

Essential chromosomal genes in *K. pneumoniae* ECL8

To classify a gene as essential or non-essential, the number of transposon insertions within each gene on the chromosome and plasmid was normalized for gene length and this value was denoted the gene insertion-index score (Figure 1C). Insertion index scores (IIS) for the *K. pneumoniae* genome followed a bimodal distribution, as has been previously described (Figure S3) [28, 42]. The probability of a gene being essential was calculated by determining the likelihood of each given insertion-index score as belonging to the essential or non-essential mode. The ratio of the IIS values was denoted the log-likelihood ratio (Log_2-LR), a metric previously used to categorize genes into essential or non-essential groupings [28, 42]. To limit the number of false-positive hits identified, genes were classified as essential only if they were 12-times more likely to be within the essential, rather than the non-essential mode. Based on the above criteria, 373 chromosomal genes were assigned a log_2-LR of less than -3.6 and were therefore classified as essential for growth on solid LB medium supplemented with kanamycin (Figure 1D). It should be noted that non-coding sequences such as tRNA and rRNA were excluded from this analysis. Most genes (4551) were classified as non-essential (Figure

311 1E). A subset of 241 genes were located between these two modes with their essentiality
312 mode was deemed 'unclear' (Figure 1F).
313
314 To understand the essential gene functions, we evaluated their COG (cluster of orthologous)
315 categories; a metric that predicts functional classification against a database of known
316 proteins. We applied a $\log_2$ COG enrichment index to identify COG categories that were
317 enriched among the essential genes in contrast to the wider genome eggNOG (v5.0) orthology
318 data [48] (Figure S4). We identified no essential genes within the COG categories for
319 chromatin structure and dynamics (B), cell motility (N) and secondary structure (Q) suggesting
320 genes within these categories are not required or redundant for *K. pneumoniae* growth in the
321 utilized nutrient-rich liquid medium. However, genes involved in signal transduction (T) and
322 inorganic ion transport/metabolism (P) were depleted, while genes involved in translation (J),
323 cell cycle control (D) and co-enzyme metabolism (H) were the most highly enriched. This
324 correlates with enriched COG categories shared among essential genes in other members of
325 the Proteobacteria such as *Salmonella enterica* Typhimurium, *S. enterica* Typhi and
326 *Caulobacter crescentus* and serves as an internal control for the validity of the library [49-51].
327
328 **"Essential" plasmid genes**
329 The identification of eleven genes on the *K. pneumoniae* ECL8 plasmid that met the criteria
330 to be defined as essential was an unexpected observation (Table 2). As previously noted, the
331 bacterial copy number of the plasmid was approximated to be one. The average IIS of a gene
332 located on the plasmid and the chromosome was comparable, 0.16 and 0.11, respectively.
333 Due to the presence of a single plasmid per bacterial cell, and an observed even distribution
334 of IISs for genes located on the plasmid, the lack of insertions in the 11 genes is unlikely to be

due to gene dosage effects arising from the presence of multiple copies of the plasmid. Notably, the 11 plasmid-borne “essential” genes included *repB,* which is required for plasmid replication. Therefore, these genes are likely to be required for plasmid replication and stability and are unlikely to be essential for growth. This hypothesis is supported by previous observations that *K. pneumoniae* remains viable when large indigenous virulence plasmids are cured from the bacterium [52-54]. A complete list for all *K. pneumoniae* ECL8 bimodal essentiality categorization and their

associated statistical significance metrics are listed in Dataset S1.

Table 2: *K. pneumoniae* ECL8 plasmid-borne genes computationally deemed essential.

Locus tag	Gene	Function[a]
ecl8_05075	*repB*_1	RCR (rolling circle replication) plasmid protein
ecl8_05092	-	SidC homolog
ecl8_05094	-	DUF2509 family protein
ecl8_05096	-	NB-ARC domain-containing protein
ecl8_05104	*rcsA*_2	DNA-binding transcriptional activator RcsA
ecl8_05105	*yedA*_2	putative transporter
ecl8_05106	-	DUF2695 domain-containing protein
ecl8_05170	-	DUF305 domain-containing protein
ecl8_05205	-	NADPH dependent preQ0 reductase
ecl8_05272	-	Transposase
ecl8_05279	*sopB*	Control of plasmid partitioning

[a]Function derived from the top hit using NCBI blastN (www.blast.ncbi.nlm.nih.gov/Blast.cgi)

Insertion free regions

Using a highly saturated transposon library it is possible to not only define essential genes, but also define chromosomal regions lacking transposons that are large enough not to have occurred by chance. Previously, we described a geometric model to predict statistically significant regions of the genome that were free from transposon insertions [28]. This model indicated that with the insertion frequency calculated for this library, for a genome of 5.3 Mb, an insertion-free region (IFR) of 145 bp or greater was statistically significant (Figure S5). The size of insertion-free regions that are statistically significant for two previously published TraDIS libraries are plotted for comparison [28, 42]. A total of 667 genomic regions with insertion-free regions ≥145 bp were identified, many which correspond to the 380 essential genes identified through the bimodal analysis described earlier.

The remaining insertion free regions can be explained in several ways. First, as noted previously [28], genes that encode proteins with essential domains are often excluded from the bimodal analysis described above as much of the gene contains transposon insertions. For example, the *polA* gene was classified as "unclear" but contained, barring a single transposon insertion event, an 826-bp insertion-free region. This IFR corresponds to 275 amino acids that are predicted to encode the 5'-3' exonuclease function of the protein (Figure 1F). This region has also been shown to be required for the growth of *Escherichia coli* in laboratory conditions [55, 56]. In contrast, but as noted for *E. coli polA*, multiple transposon insertions are present in the remaining portion of the gene, which confers the 3'-5' proofreading and polymerase activity. Aside from those genes already identified by the bimodal analyses described above, our analyses revealed 54 additional genes with statistically significant IFRs, which indicates that they are likely essential for growth under the conditions tested here. Thus, our data suggest *K. pneumoniae* contains at least 427 essential genes, which we define as the ECL8 curated essential gene list.

An explanation for the remaining IFRs can be derived from traditional bioinformatic approaches to genome annotation. Originally, genome annotation protocols overlooked small ORFs because (i) they only consider genes that code for proteins >100 amino acids, and (ii) define genes based on sequence homology to those that have been previously annotated [57-59]. Interestingly, the methodology used here revealed 59 regions ≥145 bp that lacked transposon insertion sites and did not map to within annotated CDS boundaries (Figure 1G). The applied approach is conservative and does not include insertion free regions that overlap with the 5' or 3' region of any annotated CDS. Forty-six of these regions contain potential open reading frames that could encode proteins. These putative unannotated ORFs were not

383 characterized further within this study but might represent essential genes. This study
384 emphasizes the untapped potential of TraDIS datasets to identify previously uncharacterized,
385 essential, small coding sequences and promoter elements that are not immediately obvious
386 by traditional and computational genomic annotation methods. A complete list of IFRs, within
387 annotated ORFs or in intergenic regions, and an ECL8 curated essential gene list is found in
388 Dataset S2.
389
390 **Directional insertion bias of Tn5 transposon into capsular polysaccharide (*cps*) operon**
391 As reported previously [28, 60], due to the design of the transposon used in this study,
392 transcription of polycistronic operons can be affected by the insertion orientation of the
393 transposon (Figure 2A). Directional insertion bias of the transposon was noted within a large
394 genomic region of ~14 kb encoding the virulence-associated capsular polysaccharide (*cps)*
395 operon (Figure 2B). The bioinformatic web-tool 'Kaptive' determined with high confidence
396 the *K. pneumoniae* ECL8 *cps* operon encodes for a KL2/K2 capsule with 18/18 of the expected
397 genes (Dataset S6) [61].
398
399 Notably, transposon insertions were poorly tolerated in the forward Tn orientation of the
400 DNA strand. While bias for Tn insertions has previously been described in individual genes
401 (e.g. ribosomal RNA genes), this study is the first to describe such a large bias across an operon
402 [28, 49]. However, the basis for this bias is not fully understood. One potential explanation
403 for such bias might be the presence of a gene encoding a toxic small RNA (tsRNA). Typically,
404 tsRNAs are usually present in the 5' or 3' untranslated regions of genes and act as regulators
405 of gene expression at a post-transcriptional level, but due to their small size, typically <500
406 nucleotides, they are very difficult to predict [62, 63]. However, this hypothesis does not

explain why transposon insertions are uniformly absent for the reverse orientation of the transposon and not isolated to 'hotspots' in the 5' and 3' untranslated regions. An alternative hypothesis is that the reverse orientation expression of the capsular operon might result in the accumulation of intracellular capsular intermediates that may be toxic if left to accumulate in the periplasm. This finding may hint to a more cryptic regulation mechanism of the *cps* operon with implications for other similar *Klebsiella* capsular serotypes and species.

Comparison of essential genes to other *K. pneumoniae* transposon libraries

Transposon libraries have previously been generated in other *K. pneumoniae* strains, however these studies primarily focused on identifying genes that are required for a specific phenotype i.e antibiotic stress or capsular mutants, and therefore they lack a definitive list of essential genes for *in vitro* growth [64-68]. To benchmark our library, we compared our data to previously published studies that did report *K. pneumoniae* essential gene lists: KPNIH1 (ST258), RH201207 (ST258) and ATCC 43816 (ST493) [31, 69]. As shown in Table 3, our transposon mutant library is amongst the most saturated *K. pneumoniae* libraries reported to date, permitting accurate determination of gene essentiality and delineating between real and stochastic effects. The number of essential genes among the four strains ranged from 434 to 642; a complete list and comparison of our curated gene list against the reported gene lists of KPNIH1, RH201207 and ATCC 43816 is found in Dataset S3. We speculate that the higher number of essential genes predicted in the KPNIH1 gene list is due to a lower transposon density, as this is associated with an increased likelihood of false-positive results [70]. This might be due in part to differences in the techniques used to construct the libraries; here we used a mini-Tn5 transposon which showed no bias in insertion whereas others have used the TnSeq method relying on the Himar I Mariner transposon, which has a requirement for a TA

dinucleotide motif [71]. Differences in gene essentiality might also be due to inherent genomic differences or due to differences in experimental methodology, computational approaches, or the stringency of analysis used to categorize these genes. While further validation experiments will be required to determine whether specific genes are essential, 57% of the essential genes identified in *K. pneumoniae* ECL8 were essential in the other three strains and a further 13% were shared across at least two of the three strains. Thus, these data indicate that our transposon library is sufficiently dense and representative of *K. pneumoniae* to be used for further studies.

Table 3: Comparison of *K. pneumoniae* ECL8 essential gene list with other selected studies

Strain and ST	Chromosome length (bp)	UIPs	Total essential genes	Homolog essential in ECL8[a]	Essential, no homolog in ECL8	Reference
ECL8 (ST375)	5,307,154	499,919	427[b]	245[c]	27[d]	This study
KPNIH1 (ST258)	5,394,056	41,769	642	297	103	[31]
RH201207 (ST258)	5,475,790	510,834	608	172	227	[64, 69]
ATCC 43816 (ST493)	5,374,835	415,608	476	308	121	[65, 69]

[a] Listed as essential in the referenced study, but corresponding ECL8 homolog was deemed non-essential (E-value >1e-10, nucleotide percent identity >90).
[b] Curated essential chromosomal gene number: bimodal analysis (n=373) + manual analysis of "unclear" genes with IFR (n=54).
[c] A total of 245 genes deemed essential in ECL8 with homolog(s) present in the reported essential gene lists of KPNIH1, RH201207, ATCC43816.
[d] A total of 27 essential genes were identified in ECL8 with no homolog in KPNIH1, RH201207, ATCC43816 (E-value >1e-10, nucleotide percent identity >90)

Identification of genes required for growth in human urine

TIS has become a formidable tool for rapid genome-scale screens to link genotype to phenotype. As the urinary tract is a major site for *K. pneumoniae* infection, we used our transposon mutant library to identify genes required for growth in urine, thus enabling us to define the urinome of *K. pneumoniae*. Cultures were grown until late stationary phase (12 h) followed by two subsequent 12 h passages before sequencing (Figure 3A). This approach eliminated mutants that were unable to grow in urine while allowing those capable of growth to flourish. DNA from test and control samples was harvested, sequenced, and analyzed as before (Figure S6). As the gene IISs for the library passaged in both LB and urine were highly correlated with respective biological replicates of 0.8483 and 0.9078 R^2, replicates were combined for downstream analyses (Figure S7). The data for all *K. pneumoniae* genes and their associated statistical significance metrics are listed in Dataset S4.

Ten genes that satisfied a stringent threshold of a $\log_2$ fold change ($\log_2$FC) >-2 and a Q-value ≤0.05, relative to the LB control, were considered as advantageous for *K. pneumoniae* ECL8

466 growth in urine (Figure 3B). The transposon insertion profiles of these genes showed a marked
467 decrease in overall insertions following passaging in urine when compared to the LB control
468 (Figure 3C-F), suggesting loss of these genes confers a fitness defect. These included genes
469 encoding the superoxide dismutase SodA, the structural outer membrane protein OmpA (63),
470 the periplasmic chaperone Skp [72], and five proteins (*fepB*, *fepD*, *fepG*, *exbB* and *exbD*)
471 associated with iron acquisition [73]. The remaining two genes (*ytfL* and *argH*) play key roles
472 in controlling cytoplasmic cadaverine and putrescine concentrations and amino acid
473 biosynthesis, respectively [74, 75]. The proper regulation of cadaverine and putrescine
474 maintains intracellular pH concentrations and reduce oxidative damage to proteins and DNA
475 and may be in response to acidic conditions in urine known to be unconducive for colonization
476 of uropathogens [76, 77].
477
478 To experimentally validate our observations, seven independent mutants were constructed
479 by allelic replacement of the chromosomal gene with a kanamycin (*aph*) cassette. To
480 determine whether *K. pneumoniae* strains lacking the genes identified in this screen were
481 truly less fit in urine compared to the parent strain, the WT ECL8 and individual isogenic
482 mutant strains were inoculated into urine or LB medium at a 1:1 ratio. These cultures were
483 sequentially passaged, and the CFU/mL of both the WT and mutant strain were determined
484 over a time-course of three 12 h passages (Figure 3G). When compared to the wild-type, a
485 Δ*sodA*::*aph* mutant was less fit in both urine and LB, but the phenotype was exacerbated in
486 urine. In contrast, the fitness of the remaining mutants was comparable to the parent strain
487 when grown in LB medium and only less fit when grown in urine. While the relative
488 competitive index of the Δ*ytfL*::*aph* strain was 0.8 in urine, the *ompA*, *fepB*, *fepD*, *exbB* and
489 *exbD* mutants were dramatically less fit than the parent strain in urine (Figure 3G).

Based on these observations, we hypothesized that iron-levels were limiting growth in human urine and that the ability to acquire iron was crucial for *K. pneumoniae* to survive and grow *in vivo* [78, 79]. To test this hypothesis, urine was supplemented with exogenous ferrous iron (100 µM $FeSO_4$) or an iron chelator (100 µM bipyridine/2,2-dipyridyl). No variance in optical density was observed after passaging in LB medium (Figure 4A). However, the optical density of *K. pneumoniae* cultures decreased after passage in urine (Figure 4B), and the restricted growth was further exacerbated by the addition of the iron chelator 2,2-dipyridyl (Figure 4C). In contrast, supplementation of urine with exogenous iron increased growth relative to non-supplemented cultures with no difference in growth upon passage (Figure 4D). Surprisingly, several siderophore synthesis genes did not confer a statistically significant fitness advantage for growth in urine (i.e. *entACDF*, Figure 4E). In contrast, the highest Log_2FC increase (~7-fold) in read counts mapped to the Ferric Uptake Regulator (*fur*) gene indicating its loss is beneficial for growth in urine. In Gram-negative bacteria, Fur is a key regulator for iron homeostasis functioning as a transcriptional repressor for siderophore synthesis genes in an iron concentration-dependent manner [80-82]. Furthermore, the Fur regulon includes the cognate ferric enterobactin uptake (Fep) genes, for which decreased Log_2FC read counts were also noted (Figure 4F). Altogether, this suggests that the Fur regulon plays a pivotal role for *K. pneumoniae* growth in urine by tightly regulating enterobactin synthesis and enterobactin-mediated iron uptake.

Identification of genes required for resistance to complement-mediated killing

To identify genes that protect against complement-mediated killing (previously defined as the serum resistome [23, 24], we first established the serum killing kinetics of *K. pneumoniae*

514 ECL8. Approximately, 2 x 10^8 cells were incubated with 100 µL of human serum for 180 min.
515 At specified time points, aliquots were plated to determine the number of viable bacteria. As
516 expected, no viable bacteria were recovered from the *E. coli* BW25113 control [83]. In
517 contrast, a 2 $\log_{10}$ decrease in the number of viable *K. pneumoniae* cells was observed after
518 90 min exposure to normal human serum, and a >4 $\log_{10}$ decrease after 180 min exposure. To
519 determine whether the observed reduction in viable cells was due to the presence of active
520 complement proteins, a heat-inactivated serum control was included (Figure S8).
521
522 Subsequently, 2 x 10^8 cells from the ECL8 TraDIS library were inoculated into 1 mL of human
523 serum or 1 mL of heat-inactivated human serum and incubated for 90 min. Following
524 exposure to serum, cells were grown in duplicate to an OD_{600} of 1 in LB medium to enrich for
525 viable mutants. DNA was harvested from each sample, and subsequently sequenced as
526 described previously (Figure 5A). The Pearson correlation coefficient (R^2) of gene insertion
527 index scores (IIS) for two sequenced biological replicates were calculated as 0.91 (normal
528 human serum) and 0.76 (heat inactivated serum) (Figure S9). To ensure robust data analysis,
529 thresholds were applied to the data where genes with less than 50 mapped reads in the input
530 library were removed from downstream analysis to minimize the effect of the stochastic loss
531 of mutants on downstream analysis. A total of 356 genes with a $\log_2$FC ≤-2, P<0.05, and Q-
532 value of ≤0.05 between the serum and heat-inactivated control were classified as genes that
533 are advantageous for growth under complement-mediated killing conditions (Figure 5B). The
534 complete list of all genes analyzed for growth in human serum and their associated statistical
535 significance metrics are listed in Dataset S5. The operons encoding lipopolysaccharide (LPS)
536 core antigen, O-antigen, and enterobacterial common antigen (ECA) biosynthesis were noted
537 as containing several conditionally essential genes (Figure 5C). Mutants defective in these cell

envelope structures have previously been reported to play a role in membrane integrity and resistance to serum-killing for a variety of Gram-negative bacteria [84-86]. Genes implicated as important for serum resistance encode proteins with an important role in membrane stability. They include GalE involved in LPS sugar sub-unit biosynthesis [87, 88], outer membrane protein MlaA involved in phospholipid retrograde transport [89], cardiolipin synthase ClsA [90], Bam complex component BamE [91], and proteins involved in LPS biosynthesis (LpxC) and its regulator (YejM) [92].

To validate our observations, we selected the gene with the greatest Log_2FC decrease between serum and a heat-inactivated control; a putative glycosyltransferase *espE*_3/*wbbY* (inset, Figure 5B). Analyses using the 'Kaptive' webtool suggested that ECL8 encodes the O-antigen serotype O1v2 with the operon having 98.98% nucleotide identity to the reference genome (Dataset S6) [61]. The O-antigen of the O1v2 serotype features distal repeating D-galactan I and D-galactan II sugar sub-units [93]. Despite its role in O-antigen biosynthesis, *wbbY* is not located within the *rfb* LPS operon. A previous study reported that its deletion in *K. pneumoniae* NTUH-K2044 (ST23) resulted in abrogated D-galactan II production. To determine the role of *wbbY* in serum sensitivity, the gene was replaced with an *aph* cassette and the resulting mutant was compared to its parent strain using a serum bactericidal assay. A comparable growth profile was observed for *K. pneumoniae* ECL8 and the Δ*wbbY*::*aph* mutant in LB medium (Figure 5D). However, the Δ*wbbY*::*aph* mutant was more sensitive to human serum than the parent with no viable mutants surviving after 30 min (Figure 5E). To investigate whether the *wbbY* deletion affected LPS production, crude LPS extracts were visualized using silver staining (Figure 5F). The Δ*wbbY*::*aph* strain produced LPS with a lower molecular-weight compared to the parent strain, suggesting that a truncated O-antigen was

expressed. Alterations in the amount or length of LPS produced are known to influence susceptibility to serum mediated killing [85].

Identification of genes required for serum-resistance

Following the identification of genes that when mutated confer increased sensitivity to complement-mediated killing (i.e. the serum resistome), the *K. pneumoniae* ECL8 TraDIS library was screened for mutants that confer increased resistance to serum-killing. Approximately 2 x 10^8 TraDIS mutants were incubated in 1 mL of human serum for 180 min. The output pool was washed with PBS and plated onto LB agar supplemented with kanamycin (Figure 6A). Following overnight growth, ~150,000 colonies were recovered and pooled for sequencing confirming good correlation of replicates (Figure S10). We then used AlbaTraDIS to identify mutations that conferred a fitness advantage or disadvantage for survival in serum. In addition to identifying genes with an increase or decrease in reads between the condition and control samples, AlbaTraDIS will also analyze changes in sequencing read depth of insertions immediately upstream and downstream of a gene, as well as within-gene transposon orientation biases. Such differences can be strong indicators of mutations that result in gene expression or regulatory effects (For a detailed explanation please see [45]). The data for insertions with a significant (>2-fold) change in read-depth following serum exposure for 180 min are listed in Dataset S7. Genes with the greatest significance in decreased insertions, suggesting decreased fitness, were O-antigen outer-core biosynthesis gene espJ_2/*wabI* and O-antigen ligase rfaL/*waaL* (Figure 6B). Genes with significantly increased insertions, suggesting increased fitness, included *hns*, *gnd* and *igaA* (Figure 6C). Closer inspection of the transposon insertion profiles further confirmed the enrichment of *hns* mutants when comparing the serum exposed test to the input control (Figure 6D). To

validate our observations, a defined *hns* mutant was constructed by allelic replacement with an *aph* cassette in the same orientation as native gene transcription. A comparable growth profile in LB was observed for the *hns* mutant relative to the parent (Figure 6C). To determine whether the *hns* mutant was indeed more resistant to serum a sample of 1 x 10^8 cells was incubated in serum for 360 min. At 30 min post-incubation the number of viable *hns*::aph cells was decreased by ~2 log. However, no additional decrease in viable cell numbers was observed at later time points and these strains proliferated in serum (Figure 6F). Ares and colleagues demonstrated that *rcsA; galF; wzi;* and *manC* were derepressed in a Δ*hns K. pneumoniae* mutant resulting in increased capsule production [94]. Similarly, up-regulation of *rcsA* was noted in an *E. coli* Δ*hns* mutant. RcsA is known to positively regulate the capsular locus [95, 96]. Notably, IgaA represses the Rcs regulon, preventing activation of RcsA. Mutants in *igaA* are enriched in our experiments. These data suggest that activation of the Rcs regulon confers resistance to serum killing in *K. pneumoniae*, as noted for other members of the *Enterobacteriaceae*, by increasing capsule production [97].

The *gnd* gene encodes a 6-phosphogluconate dehydrogenase involved in the oxidative branch of the pentose phosphate pathway. Interestingly, sequence reads mapping to *gnd* were enriched for the forward orientation of the transposon only (Figure S11). Transposon insertions in this orientation have transcriptional read-through driving expression of the downstream neighboring gene *manC* and more distal O-antigen biosynthesis genes (i.e. *rfb* cluster) [98]. The *manC* gene encodes mannose-1-phosphate guanylyltransferase that is required for the synthesis of capsule, and as noted above, upregulation of *manC* results in increased production of capsule.

Conclusion

For a variety of reasons, the determination of gene essentiality from TraDIS data is challenging. Here, we used two different computational approaches to identify essential genes ensuring that our essential gene dataset includes those genes that can tolerate insertions in regions of the gene but where specific domains are essential for growth. The observation that 57% of the essential genes identified in this study were found to be essential in three of the four *K. pneumoniae* TraDIS libraries described to date provides reassurance that this library would provide meaningful data for subsequent studies. Furthermore, the high density of insertion sites achieved in our study ensured reliable identification of essential and conditionally-essential genes and a low probability of false positive identification, which had previously been noted for low complexity libraries [70].

The search for genetic determinants of bacterial survival and growth *in vivo* has been augmented by whole genome approaches to infection, including transposon insertion site sequencing techniques such as TraDIS and TnSeq [16]. These data have potential implications for the design and development of novel drugs, vaccines and antivirulence strategies. In this study, we employed TraDIS to identify genes which, when mutated, confer decreased or increased fitness for growth in human urine and serum, two *in vivo* niches relevant to *K. pneumoniae* infection. Surprisingly, our study revealed 11 genes significantly required for growth in urine. These included genes encoding the outer membrane protein OmpA, its chaperone Skp, the superoxide dismutase SodA, and genes required for iron acquisition by the enterobactin uptake system. Notably, not all the genes for enterobactin synthesis, export and uptake were essential (Fig. 4). The gene encoding FepB, the periplasmic chaperone for the iron laden siderophore, was essential, as were *fepD* and *fepG*, which encode the inner

membrane uptake system. The TonB complex (TonB-ExbB-ExbD), which energizes the translocation of iron laden enterobactin through the FepA outer membrane pore, was also essential for growth in urine. In contrast, the genes encoding FepA, the inner membrane ATPase FepC, and the enterobactin synthesis (Ent) and export (TolC) components were not essential. These observations can be explained in two ways. First, as *K. pneumoniae* ECL8 contains paralogous copies of *fepA* (*fepA*_1 and *fepA*_2) and *fepC* (*fepC*_1 and *fepC*_2), the non-essential nature of *fepA* and *fepC* might be the result of functional redundancy. Second, as TraDIS is in principle a large-scale competition experiment between thousands of mutants, mutants lacking enterobactin (or aerobactin) synthesis and export genes can "cheat" by acquiring the siderophore released from siderophore-producing strains within the population, a phenomenon described previously [99, 100].

In contrast to the limited number of genes in the urinome, the serum resistome consisted of more than 144 genes. This number is significantly greater than reports of a recent study that defined the serum resistome of four independent *K. pneumoniae* strains [23]. While that study found 93 genes that were required for survival in one or more strains, remarkably only three genes were common to all four strains: *rfaH*, *lpp* and *arnD*. Comparison with our dataset revealed that in contrast to *rfaH, arnD* was not required for serum resistance in *K. pneumoniae* ECL8. Surprisingly, comparison of our data with the 56 genes comprising the serum resistome of the more distantly related multidrug resistant *E. coli* strain EC958 revealed 14 genes in common. The variation in the outcome of these experiments can be accounted for in different ways. First, in all cases the genes encoding O-antigen and/or capsule synthesis were required for growth in normal human serum; As the genes encoding these surface structures vary with serotype, they are not identified as common genes, though ostensibly

they have the same function Second, the methodology appears at first glance to be identical in each study (growth in the presence of serum for 90 min). However, not all strains exhibit the same killing kinetics in normal human serum. Using fixed timepoints, strains with longer killing kinetics are likely to have fewer genes identified in TraDIS experiments, whereas strains with short killing windows will have more. Third, several of the genes identified in the serum resistome of other strains were excluded from our downstream analysis as there were fewer than 50 transposon insertions in the gene following exposure to heat-inactivated serum. A case in point is the *lpp* gene. This observation indicates that *lpp* is required for *K. pneumoniae* ECL8 growth in human serum but not resistance to complement dependent killing *per se*. Fourth, the density of the library used, the level of comparative annotation, and the thresholds to define significance, all have the potential to influence the final outcome of such experiments. Finally, strain-specific features such as gene duplication events, functional redundancy in biosynthetic pathways, and the variation in the genetic complement of each strain, are likely to influence the contribution each gene makes to serum resistance.

Despite the intra and interspecies variation in the serum resistome noted above, comparison of the urinome and serum resistome of *K. pneumoniae* ECL8 revealed that mutation of five genes (*ompA*, *galE*, *exbB*, *exbD* and *sodA*) conferred reduced fitness for both growth in urine and survival in serum. The role of *exbB* and *exbD* are described above but their detection in both experimental conditions reinforces the importance of iron acquisition for infection. The major outer membrane protein OmpA identified in this study encodes a functionally pleiotropic outer membrane protein (85, 86). Notably, a role for OmpA in serum resistance has previously been described for *E. coli*, however it was not identified by TraDIS experiments investigating the serum resistome [24]. The molecular basis for this discrepancy remains

unresolved. GalE is known to play a key role in serum resistance for *E. coli* and *Salmonella* spp. [24]. The gene *galE* encodes a UDP-glucose 4-epimerase catalyzing the interconversion of UDP-D-galactose/UDP-D-glucose [87]. It has been previously reported that GalE plays a role in D-galactan II synthesis, an O1 LPS component in *K. pneumoniae* [88, 101]. These data suggest that loss of *galE* results in a modified LPS in *K. pneumoniae* resulting in increased serum susceptibility. Subsequently, the manganese-dependent superoxide dismutase SodA converts superoxide to hydrogen peroxide and oxygen to prevent DNA and other cellular damage [102, 103]. A previous study in *K. pneumoniae* has reported the inducible expression of *sodA* in a triumvirate system with *sodB* and *sodC*, expressed in response to anaerobic challenge and high-oxygen concentration [104]. These transcriptional responses might very well be present in both the microenvironments of blood vessels and the bladder, in the form of nutrient limitation and oxygen exposure [105-107]. Hence, the observed importance of *sodA* might be a consequence of elevated levels of reactive oxygen species (ROS) due to iron-acquisition and could represent a specialized metabolic adaptation for growth in these environments. Ultimately, these findings underline the interplay between bacterial iron homeostasis and oxidative stress previously reported in Gram-negative bacteria [108-111]. However, these data shine a light on cross-niche (i.e. urine and serum) genes and associated pathways as suitable drug development targets to treat *Klebsiella* infections. Finally, this library was then used to identify genes conferring serum resistance. An interesting finding was the observed transposon insertion orientation bias into *gnd.* As the downstream transcriptional unit of *gnd* are O-antigen related genes (i.e. biosynthesis and export), this in turn lends further credence to a transcriptional regulatory model where biosynthesis of O-antigen and capsule is coupled for biophysical reasons as has been previously reported [65, 112]. Collectively, these data show that O-antigen biosynthesis genes (i.e *wabI* and *waaL*) play

a contributing role in serum resistance whilst *hns* mutants were shown to be more resistant to serum killing than WT *K. pneumoniae* ECL8. However, the mechanism that underpins this resistance is still largely unknown and requires further characterization. Despite the previously described links between *hns* and the regulation of a selection of capsular genes [65, 94], this is the first report of a role for *hns* in resisting complement-mediated killing in human serum.

This genome-wide screen has identified a suite of genetic fitness-factors required for growth of *K. pneumoniae* ECL8 in human urine and serum. The defined ECL8 urinome and serum resistome gene sets from this study gene differ from other TraDIS studies, hinting that the genotype of different pathogenic lineages might only be a piece in understanding the underlying infection biology. Future studies like these but expanding to other isolates, and the lesser studied clinically relevant *K. pneumoniae* species complex (KpSc), will be imperative for the effective future development of targeted therapeutics towards this problematic pathogen.

Figures

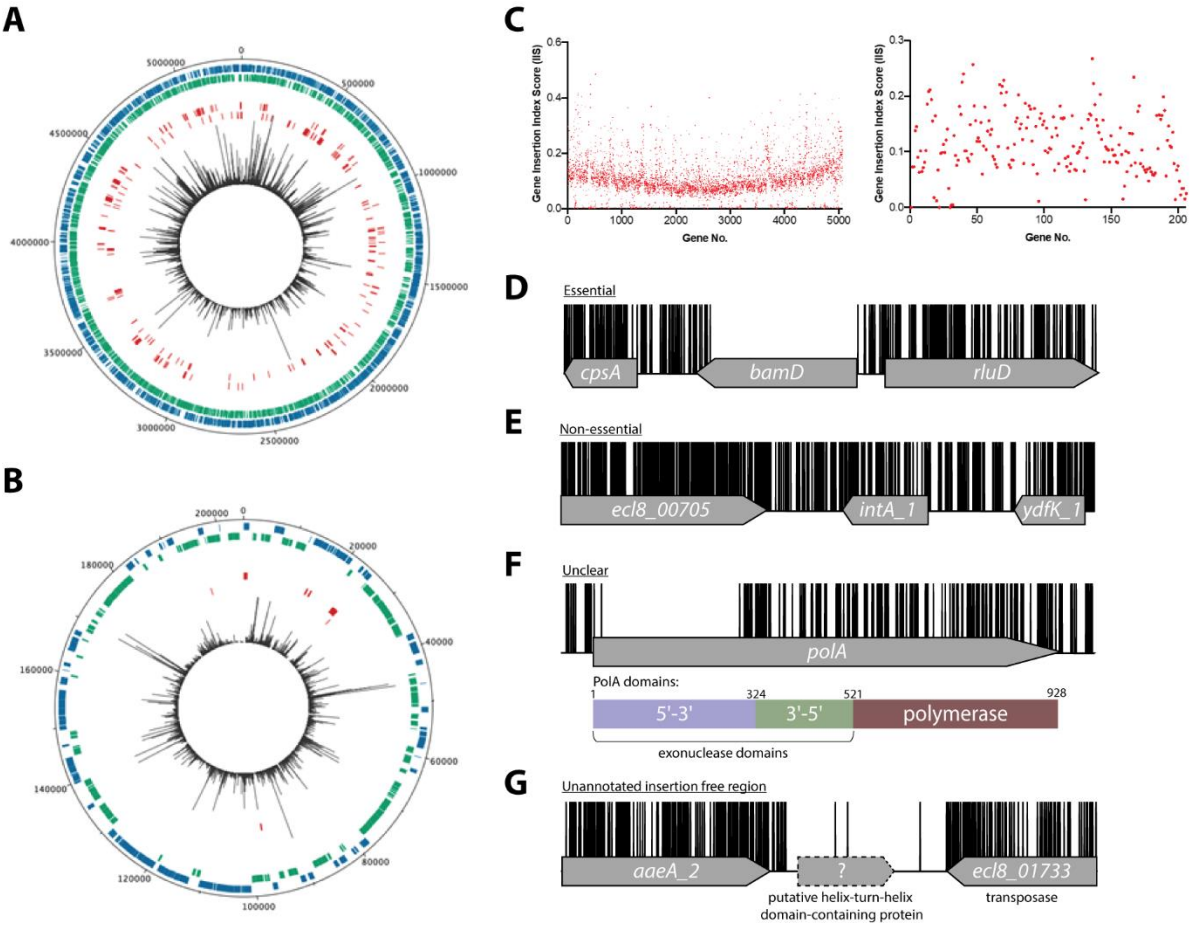

Figure 1 Overview of ECL8 TraDIS data: mapped insertions, insertion index profile and example gene insertion plots. Insertions are illustrated on the (A) Chromosome and (B) Plasmid, respectively. The outermost track displays the length of the ECL8 genome in base pairs. The subsequent two inner tracks correspond to coding sequences (CDS) on the sense (blue) and antisense (green) DNA strands, respectively. Putative essential CDSs are highlighted in red. The inner-most track (black) corresponds to the location and read frequency of transposon sequences mapped successfully to the *K. pneumoniae* ECL8 genome. Plot generated using DNAPlotter. (C) Gene insertion index scores (IIS) of the *K. pneumoniae* ECL8 TraDIS library mapped in order of genomic annotation of the *K. pneumoniae* ECL8 (left) chromosome and (right) plasmid. Example transposon insertion profiles categorised into essential, non-essential and unclear: (D) an essential gene – *bamD*, an essential outer membrane factor for β-barrel protein assembly; (E) a non-essential gene – *int*_A1, a redundant (several copies) integrase required for bacteriophage integration into the host genome; (F) an "unclear" gene – *polA* an essential gene in prokaryotes required for DNA replication but showed requirement for the N-terminal 5'-3' exonuclese domain; and (G) an insertion free region suggestive of an unannotated ORF. Transposon insertion sites are illustrated in black and capped at a maximum read depth of 1.

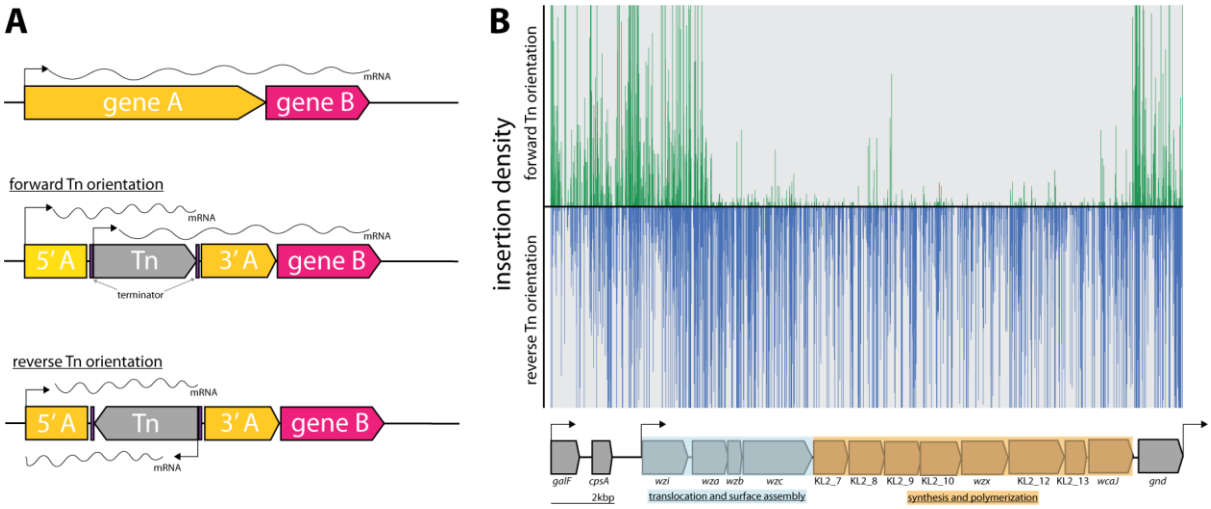

Figure 2 Directional insertion bias of transposon (Tn) into the *cps* operon. (A) Schematic representing the Tn orientation and effect on downstream transcription. The utilized Tn transposon is flanked by terminator sequences (purple) is shown inserted in gene A (yellow) of a hypothetical two-gene transcription unit AB in the forward or reverse orientation. In the forward orientation transcription of gene B (pink) is expected to occur from the promoters of 5′ of gene A or the internal Tn5 but polycistronic mRNA differs in length due to the attenuation by the terminators. (B) Transposon insertions mapping to the K2 capsular operon of *K. pneumoniae* ECL8. Transposon insertions are configured in the forward orientation (green), and reverse orientation (blue) and insertion densities are capped at a maximum read depth of 50. The operon structure of the K2 capsular genes consisting of three promoters driving the expression of three unidirectional polycistronic transcripts is depicted.

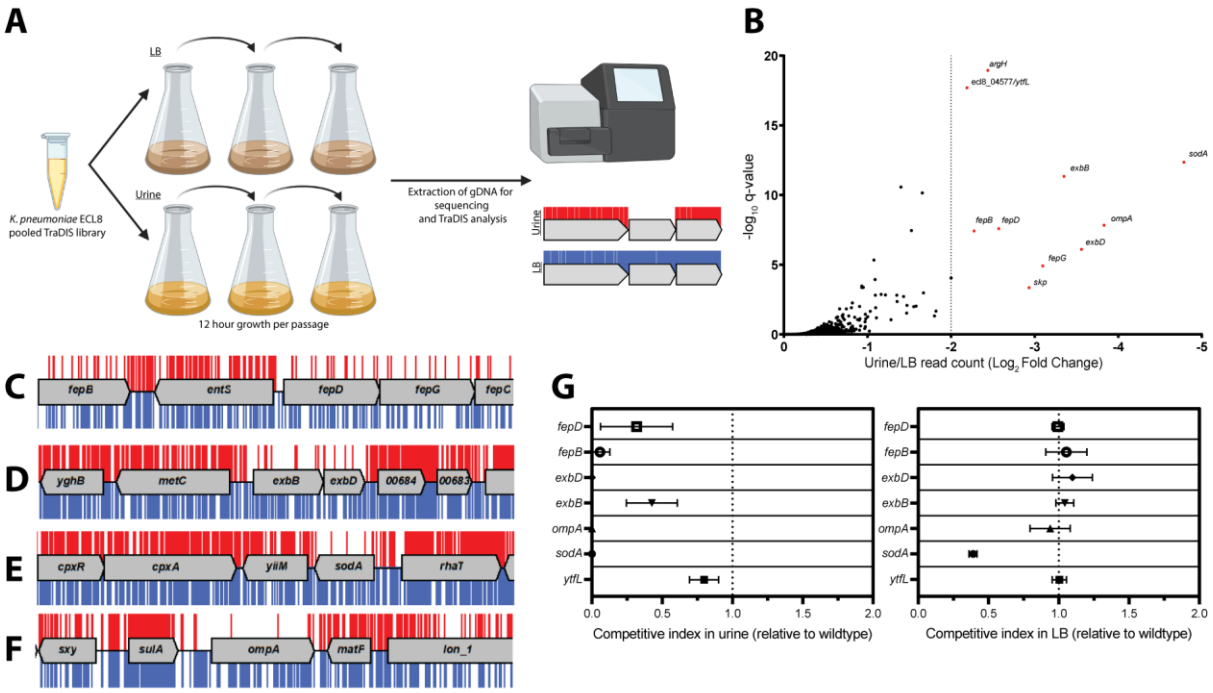

Figure 3 Overview and validation of ECL8 fitness-factors for growth in pooled human urine. (A) Schematic of the experimental design used to identify genes that provide a fitness advantage for *K. pneumoniae* ECL8 growth in pooled human urine. The *K. pneumoniae* ECL8 library was inoculated into either 50 mL of LB or 50 mL of urine and incubated at 37°C with 180 RPM shaking for 12 h. The library was passaged into 50 mL of fresh LB or pooled human urine at an initial OD_{600} of 0.05 two subsequent times. A 1 mL sample normalized to an OD_{600} of 1 from each culture was processed for genome extraction and multiplexed sequencing using an Illumina MiSeq. (B) Log_2 fold change (Log_2FC) of the read count for each *K. pneumoniae* ECL8 gene when passaged in urine relative to an LB control. Genes highlighted in red satisfy a stringent applied threshold (Log2FC >-2, Q-value ≤0.05). The Q-value is the P-value that has been adjusted for the false discovery rate for each gene. For brevity, only genes with a Log2FC ≥0 are illustrated. Selected transposon insertion profiles of genes identified as advantageous for growth in urine: (C) *fepB, fepD, fepG* (D) *exbB, exbD* (E) *sodA* and (F) *ompA*. These genes exhibited a significant loss of transposon insertions following growth in urine (red) in comparison to LB broth (blue). A 5-kb genomic region including the gene is illustrated. Reads are capped at a maximum depth of 1. (G) The fitness of gene replacement mutants relative to WT *K. pneumoniae* ECL8 in either LB medium or urine. The relative competitive index of single-gene replacement mutants after 12 h passages ×3 in either LB medium or urine. A relative fitness of one would indicate comparable fitness to WT. The mean is plotted (± 1 SD).

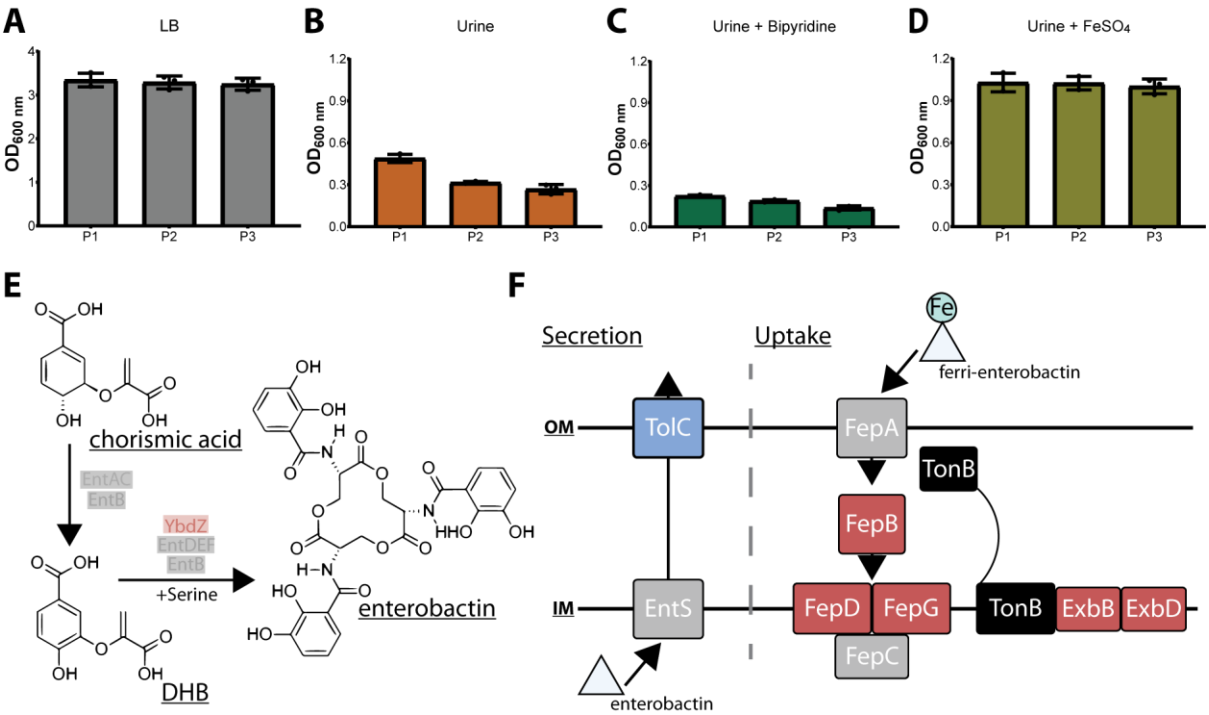

Figure 4 Growth of the *K. pneumoniae* TraDIS library following passaging in LB and urine and schematic diagrams of enterobactin synthesis, secretion and uptake. The OD_{600} of the *K. pneumoniae* TraDIS library following 12 h of growth (P1) and two sequential 12 h passages (P2 and P3). The library was passaged into fresh medium (A) LB or (B) urine to an initial OD_{600} of 0.05. To determine the effect of iron supplementation and depletion, urine was supplemented with exogenous iron (C) 100 µM $FeSO_4$ or an iron chelator (D) 100 µM 2,2-dipyridyl. The average OD_{600} of three biological replicates for each time point is plotted (±) 1 SD. (E) Simplified schematic of the enterobactin synthesis pathway. YbdZ, a co-factor of EntF for the terminal steps for enterobactin synthesis, depicted in light red had a Log_2FC sequence read value of -1.58 suggesting this gene conferred an overall fitness advantage for growth in urine. (F) Schematic representation of enterobactin secretion and uptake. The TonB transport system is present in Gram-negative bacteria and is required to transport Fe-bound enterobactin through the outer (OM) and inner membrane (IM) to the cytosol where it can be utilized. Based on Log_2FC sequence read value, loss of TolC (blue) was beneficial for growth, relative to an LB control. Loss of proteins, colored in red, had Log_2FC sequence read values <-2 suggesting they confer a fitness advantage for grown in urine. Proteins depicted in grey were genes that had Log_2FC values that ranged from -1 to 1 exposed to urine relative to an LB control. Genes depicted in black were essential and had no determinable Log_2FC value.

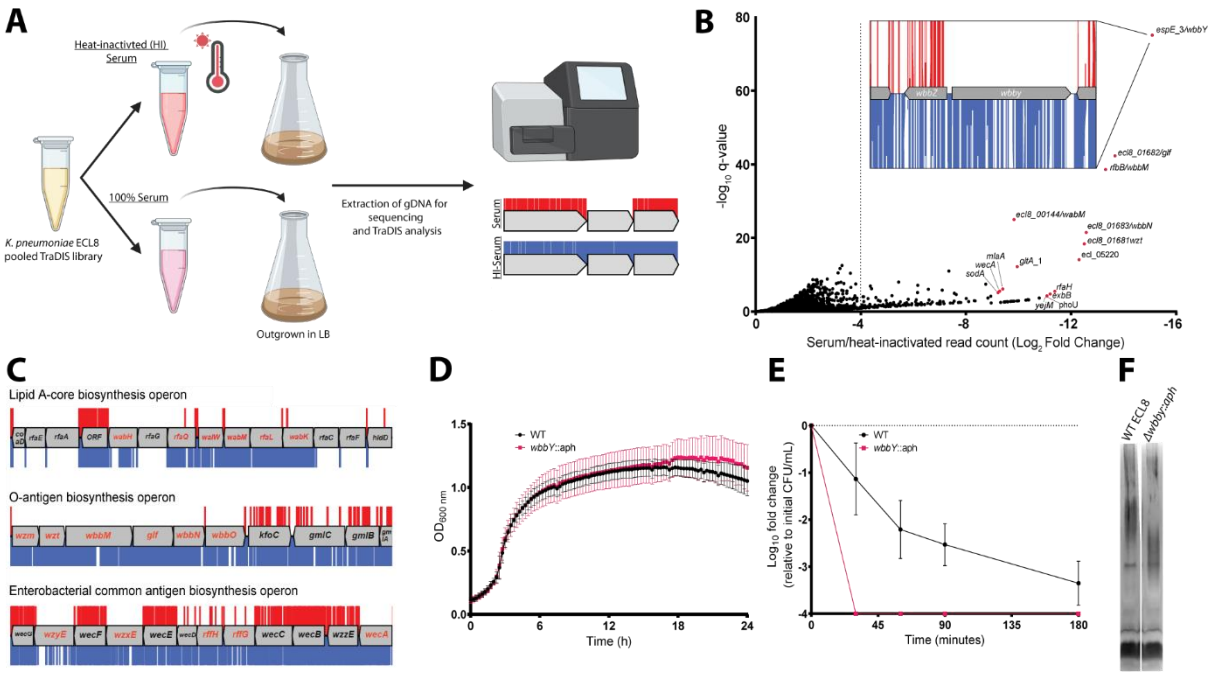

Figure 5 Overview and validation of ECL8 fitness-factors for survival in pooled human serum. (A) The experimental methodology utilized for screening the TraDIS library in human serum and a heat-inactivated serum control. *K. pneumoniae* ECL8 ($2x10^8$ cells) of the mutant library was inoculated into either 1 mL of human serum or 1 mL of heat-inactivated human serum and incubated for 90 min. Following exposure to serum, cells were grown to an OD_{600} of 1 in LB medium to enrich for viable mutants. A 1 mL sample normalized to an OD_{600} of 1 from each culture was processed for genome extraction and multiplexed sequencing using an Illumina MiSeq. (B) Log_2FC for each gene of the *K. pneumoniae* ECL8 TraDIS library when incubated in pooled human serum relative to a heat-inactivated serum control. Selected genes highlighted in red are amongst the total of 144 genes that satisfy a stringent applied threshold ($Log_2FC \geq -4$, Q-value ≤0.05). For brevity, only genes with a $Log_2FC \geq 0$ are illustrated. Inset: transposon insertion profile of *wbbY*, gene with the highest fold Log_2FC, flanked by *wbbZ* and a transposable element at its 3'. Transposon insertions following exposure to serum and a heat-inactivated serum control are illustrated in red and blue, respectively. Transposon reads have been capped at a maximum of 10. (C) Transposon insertion profiles of genes within the: LPS, O-antigen and the ECA biosynthesis operons. Genes in red font had a significantly ($Log_2FC = \geq -4$, Q-Value = ≤0.05) decreased fitness when disrupted with a transposon following exposure to serum for 90 minute (red), relative to a heat-inactivated serum control (blue). Operons are not drawn to scale and reads capped at a maximum read depth of 1. (D) Growth profile of WT *K. pneumoniae* ECL8 and Δ*wbby*::*aph* in LB broth. Mean is plotted (± 1 SD). (E) Serum killing assay of WT *K. pneumoniae* ECL8 and Δ*wbby*::*aph.* Mean is plotted (± 1 SD). (F) LPS profiles of WT *K. pneumoniae* ECL8 and Δ*wbby*::*aph*. Overnight cultures of each strain were normalised to an OD_{600} of 1. The LPS was separated on 4-12% Bis-Tris gels and was visualized by silver staining using the SilverQuest kit (Invitrogen).

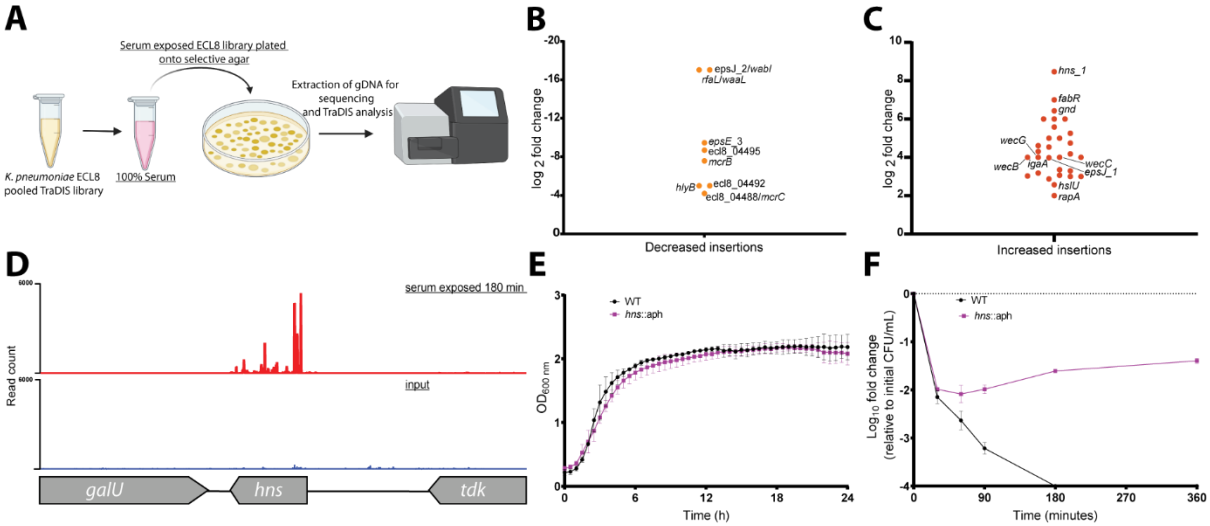

Figure 6 Overview and validation of ECL8 genes that increase resistance to complement-mediated killing. (A) The experimental methodology utilized for screening the TraDIS library to identify genetic factors that increase resistance to human serum. *K. pneumoniae* ECL8 (2×10^8 cells) of the mutant library was inoculated into 1 mL of human serum and incubated for 180 min and compared to before serum exposure input control. The output pool was washed with PBS and plated onto LB agar supplemented with kanamycin. Following overnight growth, ~150,000 colonies were recovered and pooled for sequencing. Comparative analysis using AlbaTraDIS software depicting genes with (B) decreased insertions suggesting a loss of fitness or (C) increased insertions suggesting a gain of fitness to serum exposure. (D) Transposon and read count insertion profiles of *hns* locus: red illustrating pooled mutant serum exposed for 180 min and blue denoting the before serum exposure input control. (E) Growth profile of WT K. pneumoniae ECL8 and Δ*hns*::*aph* in LB broth. Mean is plotted (± 1 SD), where n=3. (F) Serum killing assay of WT *K. pneumoniae ECL8* and Δ*hns*::*aph*. Mean is plotted (± 1 SD), where n=3.

Supporting information captions

Figure S1: (A) Pearson correlation coefficient (R2) of gene insertion index scores (IIS) of two sequenced technical replicates of the Klebsiella pneumoniae ECL8 TraDIS library (KTL1 and KTL2). The IIS of genes located on the chromosome and plasmid are highlighted in blue and red respectively. (B) Number of unique reads identified (%) in the raw fastQ file of the *K. pneumoniae* TraDIS library in sequentially larger k-mer pools up to three million reads. Plot generated using BBTools: bbcountunique.sh in non-cumulative mode (https://jgi.doe.gov/data-and-tools/bbtools/)

Figure S2 Sequencing depth of the *K. pneumoniae* ECL8 plasmid (black) relative to the *K. pneumoniae* ECL8 chromosome (green). The plasmid has a read depth 1.33x that of the genome suggesting the plasmid has a copy number of one. Figure generated using Bandage (v3).

Figure S3 The frequency distribution of insertion index scores. The insertion index score for each coding sequence was calculated as the number of insertions per CDS divided by the CDS length in base pairs to normalize for gene length. An exponential distribution model was fitted to the left mode that includes essential genes, and a gamma distribution model was fitted to the right, nonessential mode (blue). For a given insertion index score, the probability of belonging to each mode was calculated, and the ratio of these values was the log likelihood score. A gene was classified as essential if its log likelihood score was less than $\log_2 12$ and was therefore 12 times more likely to belong to the red mode than the blue mode.

Figure S4 The COG Enrichment index comprising 373 genes classified as essential in *K. pneumoniae* ECL8. This index is calculated as the percentage of the essential genome made up of a COG divided by the percentage of the whole genome made up by the same COG. The $\log^2$ fold enrichment is displayed, and significant differences were calculated using the two-tailed Fisher's exact test. Annotations were computed using eggnog-mapper based on eggNOG orthology data (2)

Figure S5 Mathematical simulation (10^5 instances) of random transposon insertion events under the null model of random insertion previously described (3). The probability of at least one insertion free region (IFR) of length (l) occurring in a genome of 5.3 Mb containing 554,834 transposon insertions (blue). Genome length and no. of genome-wide insertions from TraDIS studies by Langridge *et al.,* 2012 and Goodall *et al.,* 2018 plotted for comparison (3, 4).

Figure S6 (A) Sequencing depth required to sample a given proportion of the K. pneumoniae TraDIS library. The following equation: UIPs = $s\text{-}s(\frac{s-1}{s})^n$ was applied to calculate the approximate number of sequence reads required to sample full library diversity i.e. 100% of Unique Insertion Points (UIPs). UIPs = Unique Insertion Points, n = number of mapped reads in millions (M) and s = sample size i.e. 499,919 CDS UIPs, as described in Chapter 3. (B) The approximate number of CDS UIPs represented by a given number of sequence reads (M) are shown as a percentage of the total CDS UIPs i.e. 499,919.

Figure S7 The Pearson correlation coefficient (R^2) of gene insertion index scores (IIS) for two sequenced biological replicates of the *K. pneumoniae* ECL8 TraDIS library following thee 12 h passages in (blue) LB broth or (red) pooled human urine. The inline barcode identifiers used to demultiplex and distinguish replicates are highlighted in brackets ()..

Figure S8 Serum killing assay of *K. pneumoniae* ECL8 and *E. coli* BW25113. A sample of 2×10^8 bacterial cells were incubated in 100 µL of human serum (solid line) or heat-inactivated human serum (dashed line) for 180 min. Viable bacterial numbers (cfu/ml) were sampled at regular time points by plating onto LB agar, overnight incubation at 37 °C and subsequent counting of the colonies. The $\log_{10}$ fold change in viable cell number was measured. *E. coli* BW25113 lacks O-antigen and was used as a serum sensitive control. The mean of three biological replicates is shown ± 1 SD.

Figure S9 The pearson correlation coefficient (R^2) of gene insertion index scores (IIS) for two sequenced biological replicates of the *K. pneumoniae* ECL8 TraDIS library following 90 min exposure to (blue) Heat-inactivated serum or (red) Serum. The inline barcodes used to demultiplex and distinguish replicates are given in brackets ().

Figure S10 Pearson correlation coefficient (R2) of two biological replicates from the output TraDIS library following exposure to human serum for 180 min.

Figure S11 Directional insertion bias of transposon (Tn) into *gnd*. Transposon insertions configured in the forward orientation (green), reverse orientation (blue). Transposon insertion densities are capped at a maximum read depth of 2000. Below – genomic context of *gnd* with a putative promoter for *manC* driving the transcriptional unit (*rfb* cluster) for O-antigen biosynthesis.

Dataset S1 Essential gene table ECL8

Dataset S2 Insertion Free Regions (IFR) within ECL8 (LB)

Dataset S3 Essential Gene Comparison against ECL8

Dataset S4 Essential gene table ECL8 (Urine)

Dataset S5 Essential gene table ECL8 (Serum)

Dataset S6 Kaptive webserver results - ECL8 O-antigen K-antigen

Dataset S7 AlbaTraDIS ECL8 180 Serum exposure results

References

1. Bagley ST. Habitat association of Klebsiella species. Infect Control. 1985;6(2):52-8. doi: 10.1017/s0195941700062603. PubMed PMID: 3882590.
2. Holt KE, Wertheim H, Zadoks RN, Baker S, Whitehouse CA, Dance D, et al. Genomic analysis of diversity, population structure, virulence, and antimicrobial resistance in Klebsiella pneumoniae, an urgent threat to public health. Proc Natl Acad Sci U S A. 2015;112(27):E3574-81. Epub 20150622. doi: 10.1073/pnas.1501049112. PubMed PMID: 26100894; PubMed Central PMCID: PMCPMC4500264.
3. Podschun R, Ullmann U. Klebsiella spp. as nosocomial pathogens: epidemiology, taxonomy, typing methods, and pathogenicity factors. Clin Microbiol Rev. 1998;11(4):589-603. doi: 10.1128/CMR.11.4.589. PubMed PMID: 9767057; PubMed Central PMCID: PMCPMC88898.
4. Ko WC, Paterson DL, Sagnimeni AJ, Hansen DS, Von Gottberg A, Mohapatra S, et al. Community-acquired Klebsiella pneumoniae bacteremia: global differences in clinical patterns. Emerg Infect Dis. 2002;8(2):160-6. doi: 10.3201/eid0802.010025. PubMed PMID: 11897067; PubMed Central PMCID: PMCPMC2732457.
5. Goncalves Barbosa LC, Silva ESJA, Bordoni GP, Barbosa GO, Carneiro LC. Elevated Mortality Risk from CRKp Associated with Comorbidities: Systematic Review and Meta-Analysis. Antibiotics (Basel). 2022;11(7). Epub 20220629. doi: 10.3390/antibiotics11070874. PubMed PMID: 35884128; PubMed Central PMCID: PMCPMC9312274.
6. Tumbarello M, Trecarichi EM, De Rosa FG, Giannella M, Giacobbe DR, Bassetti M, et al. Infections caused by KPC-producing Klebsiella pneumoniae: differences in therapy and mortality in a multicentre study. J Antimicrob Chemother. 2015;70(7):2133-43. Epub 20150421. doi: 10.1093/jac/dkv086. PubMed PMID: 25900159.
7. Clegg S, Murphy CN. Epidemiology and Virulence of Klebsiella pneumoniae. Microbiol Spectr. 2016;4(1). doi: 10.1128/microbiolspec.UTI-0005-2012. PubMed PMID: 26999397.
8. Paczosa MK, Mecsas J. Klebsiella pneumoniae: Going on the Offense with a Strong Defense. Microbiol Mol Biol Rev. 2016;80(3):629-61. Epub 20160615. doi: 10.1128/MMBR.00078-15. PubMed PMID: 27307579; PubMed Central PMCID: PMCPMC4981674.
9. Ikuta KS, Swetschinski LR, Robles Aguilar G, Sharara F, Mestrovic T, Gray AP, et al. Global mortality associated with 33 bacterial pathogens in 2019: a systematic analysis for the Global Burden of Disease Study 2019. The Lancet. 2022;400(10369):2221-48. doi: 10.1016/S0140-6736(22)02185-7.
10. Pham MH, Hoi LT, Beale MA, Khokhar FA, Hoa NT, Musicha P, et al. Evidence of widespread endemic populations of highly multidrug resistant Klebsiella pneumoniae in hospital settings in Hanoi, Vietnam: a prospective cohort study. The Lancet Microbe. 2023;4(4):e255-e63. doi: 10.1016/S2666-5247(22)00338-X.
11. Mohd Asri NA, Ahmad S, Mohamud R, Mohd Hanafi N, Mohd Zaidi NF, Irekeola AA, et al. Global Prevalence of Nosocomial Multidrug-Resistant Klebsiella pneumoniae: A Systematic Review and Meta-Analysis. Antibiotics. 2021;10(12):1508. PubMed PMID: doi:10.3390/antibiotics10121508.
12. Navon-Venezia S, Kondratyeva K, Carattoli A. Klebsiella pneumoniae: a major worldwide source and shuttle for antibiotic resistance. FEMS Microbiol Rev. 2017;41(3):252-75. doi: 10.1093/femsre/fux013. PubMed PMID: 28521338.
13. Garbati MA, Al Godhair AI. The growing resistance of Klebsiella pneumoniae; the need to expand our antibiogram: case report and review of the literature. Afr J Infect Dis.

2013;7(1):8-10. doi: 10.4314/ajid.v7i1.2. PubMed PMID: 24381721; PubMed Central PMCID: PMCPMC3647522.
14. Campos AC, Albiero J, Ecker AB, Kuroda CM, Meirelles LE, Polato A, et al. Outbreak of Klebsiella pneumoniae carbapenemase-producing K pneumoniae: A systematic review. Am J Infect Control. 2016;44(11):1374-80. Epub 20160505. doi: 10.1016/j.ajic.2016.03.022. PubMed PMID: 27156198.
15. Rojas LJ, Salim M, Cober E, Richter SS, Perez F, Salata RA, et al. Colistin Resistance in Carbapenem-Resistant Klebsiella pneumoniae: Laboratory Detection and Impact on Mortality. Clin Infect Dis. 2017;64(6):711-8. doi: 10.1093/cid/ciw805. PubMed PMID: 27940944; PubMed Central PMCID: PMCPMC5850634.
16. Cain AK, Barquist L, Goodman AL, Paulsen IT, Parkhill J, van Opijnen T. A decade of advances in transposon-insertion sequencing. Nat Rev Genet. 2020;21(9):526-40. Epub 20200612. doi: 10.1038/s41576-020-0244-x. PubMed PMID: 32533119; PubMed Central PMCID: PMCPMC7291929.
17. Barquist L, Mayho M, Cummins C, Cain AK, Boinett CJ, Page AJ, et al. The TraDIS toolkit: sequencing and analysis for dense transposon mutant libraries. Bioinformatics. 2016;32(7):1109-11. Epub 20160121. doi: 10.1093/bioinformatics/btw022. PubMed PMID: 26794317; PubMed Central PMCID: PMCPMC4896371.
18. Wyres KL, Lam MMC, Holt KE. Population genomics of Klebsiella pneumoniae. Nat Rev Microbiol. 2020;18(6):344-59. Epub 20200213. doi: 10.1038/s41579-019-0315-1. PubMed PMID: 32055025.
19. Marques C, Menezes J, Belas A, Aboim C, Cavaco-Silva P, Trigueiro G, et al. Klebsiella pneumoniae causing urinary tract infections in companion animals and humans: population structure, antimicrobial resistance and virulence genes. J Antimicrob Chemother. 2019;74(3):594-602. doi: 10.1093/jac/dky499. PubMed PMID: 30535393.
20. Bengoechea JA, Sa Pessoa J. Klebsiella pneumoniae infection biology: living to counteract host defences. FEMS Microbiol Rev. 2019;43(2):123-44. doi: 10.1093/femsre/fuy043. PubMed PMID: 30452654; PubMed Central PMCID: PMCPMC6435446.
21. Choi M, Hegerle N, Nkeze J, Sen S, Jamindar S, Nasrin S, et al. The Diversity of Lipopolysaccharide (O) and Capsular Polysaccharide (K) Antigens of Invasive Klebsiella pneumoniae in a Multi-Country Collection. Front Microbiol. 2020;11:1249. Epub 20200612. doi: 10.3389/fmicb.2020.01249. PubMed PMID: 32595624; PubMed Central PMCID: PMCPMC7303279.
22. Martin RM, Bachman MA. Colonization, Infection, and the Accessory Genome of Klebsiella pneumoniae. Front Cell Infect Microbiol. 2018;8:4. Epub 20180122. doi: 10.3389/fcimb.2018.00004. PubMed PMID: 29404282; PubMed Central PMCID: PMCPMC5786545.
23. Short FL, Di Sario G, Reichmann NT, Kleanthous C, Parkhill J, Taylor PW. Genomic Profiling Reveals Distinct Routes To Complement Resistance in Klebsiella pneumoniae. Infect Immun. 2020;88(8). Epub 20200721. doi: 10.1128/IAI.00043-20. PubMed PMID: 32513855; PubMed Central PMCID: PMCPMC7375759.
24. Phan MD, Peters KM, Sarkar S, Lukowski SW, Allsopp LP, Gomes Moriel D, et al. The serum resistome of a globally disseminated multidrug resistant uropathogenic Escherichia coli clone. PLoS Genet. 2013;9(10):e1003834. Epub 20131003. doi: 10.1371/journal.pgen.1003834. PubMed PMID: 24098145; PubMed Central PMCID: PMCPMC3789825.
25. McCarthy AJ, Taylor PW. Analysis of Escherichia coli K1 Virulence Genes by Transposon-Directed Sequencing. Methods Mol Biol. 2022;2377:199-213. doi: 10.1007/978-1-0716-1720-5_11. PubMed PMID: 34709618.

26. Ondari EM, Klemm EJ, Msefula CL, El Ghany MA, Heath JN, Pickard DJ, et al. Rapid transcriptional responses to serum exposure are associated with sensitivity and resistance to antibody-mediated complement killing in invasive Salmonella Typhimurium ST313. Wellcome Open Res. 2019;4:74. Epub 20190425. doi: 10.12688/wellcomeopenres.15059.1. PubMed PMID: 31231691; PubMed Central PMCID: PMCPMC6560496.
27. Subashchandrabose S, Smith S, DeOrnellas V, Crepin S, Kole M, Zahdeh C, et al. Acinetobacter baumannii Genes Required for Bacterial Survival during Bloodstream Infection. mSphere. 2016;1(1). Epub 20151104. doi: 10.1128/mSphere.00013-15. PubMed PMID: 27303682; PubMed Central PMCID: PMCPMC4863628.
28. Goodall ECA, Robinson A, Johnston IG, Jabbari S, Turner KA, Cunningham AF, et al. The Essential Genome of Escherichia coli K-12. mBio. 2018;9(1). Epub 20180220. doi: 10.1128/mBio.02096-17. PubMed PMID: 29463657; PubMed Central PMCID: PMCPMC5821084.
29. Fabian BK, Foster C, Asher AJ, Elbourne LDH, Cain AK, Hassan KA, et al. Elucidating Essential Genes in Plant-Associated Pseudomonas protegens Pf-5 Using Transposon Insertion Sequencing. J Bacteriol. 2021;203(7). Epub 20210308. doi: 10.1128/JB.00432-20. PubMed PMID: 33257523; PubMed Central PMCID: PMCPMC8088517.
30. Wong YC, Abd El Ghany M, Naeem R, Lee KW, Tan YC, Pain A, et al. Candidate Essential Genes in Burkholderia cenocepacia J2315 Identified by Genome-Wide TraDIS. Front Microbiol. 2016;7:1288. Epub 20160822. doi: 10.3389/fmicb.2016.01288. PubMed PMID: 27597847; PubMed Central PMCID: PMCPMC4993015.
31. Ramage B, Erolin R, Held K, Gasper J, Weiss E, Brittnacher M, et al. Comprehensive Arrayed Transposon Mutant Library of Klebsiella pneumoniae Outbreak Strain KPNIH1. J Bacteriol. 2017;199(20). Epub 20170919. doi: 10.1128/JB.00352-17. PubMed PMID: 28760848; PubMed Central PMCID: PMCPMC5637181.
32. DeJesus MA, Gerrick ER, Xu W, Park SW, Long JE, Boutte CC, et al. Comprehensive Essentiality Analysis of the Mycobacterium tuberculosis Genome via Saturating Transposon Mutagenesis. mBio. 2017;8(1). Epub 20170117. doi: 10.1128/mBio.02133-16. PubMed PMID: 28096490; PubMed Central PMCID: PMCPMC5241402.
33. Ebert M, Laass S, Burghartz M, Petersen J, Kossmehl S, Wohlbrand L, et al. Transposon mutagenesis identified chromosomal and plasmid genes essential for adaptation of the marine bacterium Dinoroseobacter shibae to anaerobic conditions. J Bacteriol. 2013;195(20):4769-77. Epub 20130823. doi: 10.1128/JB.00860-13. PubMed PMID: 23974024; PubMed Central PMCID: PMCPMC3807425.
34. Hardy L, Juan PA, Coupat-Goutaland B, Charpentier X. Transposon Insertion Sequencing in a Clinical Isolate of Legionella pneumophila Identifies Essential Genes and Determinants of Natural Transformation. J Bacteriol. 2021;203(3). Epub 20210111. doi: 10.1128/JB.00548-20. PubMed PMID: 33168636; PubMed Central PMCID: PMCPMC7811196.
35. Armbruster CE, Forsyth-DeOrnellas V, Johnson AO, Smith SN, Zhao L, Wu W, et al. Genome-wide transposon mutagenesis of Proteus mirabilis: Essential genes, fitness factors for catheter-associated urinary tract infection, and the impact of polymicrobial infection on fitness requirements. PLoS Pathog. 2017;13(6):e1006434. Epub 20170614. doi: 10.1371/journal.ppat.1006434. PubMed PMID: 28614382; PubMed Central PMCID: PMCPMC5484520.
36. Roth M, Goodall ECA, Pullela K, Jaquet V, François P, Henderson IR, et al. Transposon-Directed Insertion-Site Sequencing Reveals Glycolysis Gene gpmA as Part of the

H(2)O(2) Defense Mechanisms in Escherichia coli. Antioxidants (Basel). 2022;11(10). Epub 20221018. doi: 10.3390/antiox11102053. PubMed PMID: 36290776; PubMed Central PMCID: PMCPMC9598634.

37. Winkle M, Hernández-Rocamora VM, Pullela K, Goodall ECA, Martorana AM, Gray J, et al. DpaA Detaches Braun's Lipoprotein from Peptidoglycan. mBio. 2021;12(3). Epub 20210504. doi: 10.1128/mBio.00836-21. PubMed PMID: 33947763; PubMed Central PMCID: PMCPMC8263019.

38. Goodall ECA, Isom GL, Rooke JL, Pullela K, Icke C, Yang Z, et al. Loss of YhcB results in dysregulation of coordinated peptidoglycan, LPS and phospholipid synthesis during Escherichia coli cell growth. PLOS Genetics. 2021;17(12):e1009586. doi: 10.1371/journal.pgen.1009586.

39. Hoashi K, Harada S, Ishii Y, Aoki K, Ishikawa S, Oshiro Y, et al. Community-acquired liver abscess caused by capsular genotype K2-ST375 hypervirulent Klebsiella pneumoniae isolates. IDCases. 2019;17:e00577. Epub 20190614. doi: 10.1016/j.idcr.2019.e00577. PubMed PMID: 31293894; PubMed Central PMCID: PMCPMC6595073.

40. Connor TR, Loman NJ, Thompson S, Smith A, Southgate J, Poplawski R, et al. CLIMB (the Cloud Infrastructure for Microbial Bioinformatics): an online resource for the medical microbiology community. Microb Genom. 2016;2(9):e000086. Epub 20160920. doi: 10.1099/mgen.0.000086. PubMed PMID: 28785418; PubMed Central PMCID: PMCPMC5537631.

41. Rutherford K, Parkhill J, Crook J, Horsnell T, Rice P, Rajandream MA, et al. Artemis: sequence visualization and annotation. Bioinformatics. 2000;16(10):944-5. doi: 10.1093/bioinformatics/16.10.944. PubMed PMID: 11120685.

42. Langridge GC, Phan MD, Turner DJ, Perkins TT, Parts L, Haase J, et al. Simultaneous assay of every Salmonella Typhi gene using one million transposon mutants. Genome Res. 2009;19(12):2308-16. Epub 20091013. doi: 10.1101/gr.097097.109. PubMed PMID: 19826075; PubMed Central PMCID: PMCPMC2792183.

43. Shen W, Le S, Li Y, Hu F. SeqKit: A Cross-Platform and Ultrafast Toolkit for FASTA/Q File Manipulation. PLoS One. 2016;11(10):e0163962. Epub 20161005. doi: 10.1371/journal.pone.0163962. PubMed PMID: 27706213; PubMed Central PMCID: PMCPMC5051824.

44. Cock PJ, Chilton JM, Gruning B, Johnson JE, Soranzo N. NCBI BLAST+ integrated into Galaxy. Gigascience. 2015;4:39. Epub 20150825. doi: 10.1186/s13742-015-0080-7. PubMed PMID: 26336600; PubMed Central PMCID: PMCPMC4557756.

45. Page AJ, Bastkowski S, Yasir M, Turner AK, Le Viet T, Savva GM, et al. AlbaTraDIS: Comparative analysis of large datasets from parallel transposon mutagenesis experiments. PLoS Comput Biol. 2020;16(7):e1007980. Epub 20200717. doi: 10.1371/journal.pcbi.1007980. PubMed PMID: 32678849; PubMed Central PMCID: PMCPMC7390408.

46. Datsenko KA, Wanner BL. One-step inactivation of chromosomal genes in Escherichia coli K-12 using PCR products. Proc Natl Acad Sci U S A. 2000;97(12):6640-5. doi: 10.1073/pnas.120163297. PubMed PMID: 10829079; PubMed Central PMCID: PMCPMC18686.

47. Wick RR, Schultz MB, Zobel J, Holt KE. Bandage: interactive visualization of de novo genome assemblies. Bioinformatics. 2015;31(20):3350-2. Epub 20150622. doi: 10.1093/bioinformatics/btv383. PubMed PMID: 26099265; PubMed Central PMCID: PMCPMC4595904.

48. Huerta-Cepas J, Szklarczyk D, Heller D, Hernandez-Plaza A, Forslund SK, Cook H, et al. eggNOG 5.0: a hierarchical, functionally and phylogenetically annotated orthology

resource based on 5090 organisms and 2502 viruses. Nucleic Acids Res. 2019;47(D1):D309-D14. doi: 10.1093/nar/gky1085. PubMed PMID: 30418610; PubMed Central PMCID: PMCPMC6324079.

49. Christen B, Abeliuk E, Collier JM, Kalogeraki VS, Passarelli B, Coller JA, et al. The essential genome of a bacterium. Mol Syst Biol. 2011;7:528. Epub 20110830. doi: 10.1038/msb.2011.58. PubMed PMID: 21878915; PubMed Central PMCID: PMCPMC3202797.

50. Grazziotin AL, Vidal NM, Venancio TM. Uncovering major genomic features of essential genes in Bacteria and a methanogenic Archaea. FEBS J. 2015;282(17):3395-411. Epub 20150714. doi: 10.1111/febs.13350. PubMed PMID: 26084810; PubMed Central PMCID: PMCPMC4558319.

51. Barquist L, Langridge GC, Turner DJ, Phan MD, Turner AK, Bateman A, et al. A comparison of dense transposon insertion libraries in the Salmonella serovars Typhi and Typhimurium. Nucleic Acids Res. 2013;41(8):4549-64. Epub 20130306. doi: 10.1093/nar/gkt148. PubMed PMID: 23470992; PubMed Central PMCID: PMCPMC3632133.

52. Tang HL, Chiang MK, Liou WJ, Chen YT, Peng HL, Chiou CS, et al. Correlation between Klebsiella pneumoniae carrying pLVPK-derived loci and abscess formation. Eur J Clin Microbiol Infect Dis. 2010;29(6):689-98. Epub 20100411. doi: 10.1007/s10096-010-0915-1. PubMed PMID: 20383552.

53. Rodriguez-Medina N, Martinez-Romero E, De la Cruz MA, Ares MA, Valdovinos-Torres H, Silva-Sanchez J, et al. A Klebsiella variicola Plasmid Confers Hypermucoviscosity-Like Phenotype and Alters Capsule Production and Virulence. Front Microbiol. 2020;11:579612. Epub 20201216. doi: 10.3389/fmicb.2020.579612. PubMed PMID: 33391198; PubMed Central PMCID: PMCPMC7772424.

54. Yang X, Dong N, Liu X, Yang C, Ye L, Chan EW, et al. Co-conjugation of Virulence Plasmid and KPC Plasmid in a Clinical Klebsiella pneumoniae Strain. Front Microbiol. 2021;12:739461. Epub 20211108. doi: 10.3389/fmicb.2021.739461. PubMed PMID: 34819921; PubMed Central PMCID: PMCPMC8606748.

55. Joyce CM, Grindley ND. Method for determining whether a gene of Escherichia coli is essential: application to the polA gene. J Bacteriol. 1984;158(2):636-43. doi: 10.1128/jb.158.2.636-643.1984. PubMed PMID: 6233260; PubMed Central PMCID: PMCPMC215477.

56. Gallagher LA, Bailey J, Manoil C. Ranking essential bacterial processes by speed of mutant death. Proc Natl Acad Sci U S A. 2020;117(30):18010-7. Epub 20200714. doi: 10.1073/pnas.2001507117. PubMed PMID: 32665440; PubMed Central PMCID: PMCPMC7395459.

57. Warren AS, Archuleta J, Feng WC, Setubal JC. Missing genes in the annotation of prokaryotic genomes. BMC Bioinformatics. 2010;11(1):131. Epub 20100315. doi: 10.1186/1471-2105-11-131. PubMed PMID: 20230630; PubMed Central PMCID: PMCPMC3098052.

58. Mat-Sharani S, Firdaus-Raih M. Computational discovery and annotation of conserved small open reading frames in fungal genomes. BMC Bioinformatics. 2019;19(Suppl 13):551. Epub 20190204. doi: 10.1186/s12859-018-2550-2. PubMed PMID: 30717662; PubMed Central PMCID: PMCPMC7394265.

59. Miravet-Verde S, Ferrar T, Espadas-Garcia G, Mazzolini R, Gharrab A, Sabido E, et al. Unraveling the hidden universe of small proteins in bacterial genomes. Mol Syst Biol. 2019;15(2):e8290. Epub 20190222. doi: 10.15252/msb.20188290. PubMed PMID: 30796087; PubMed Central PMCID: PMCPMC6385055.

60. Hutchison CA, 3rd, Merryman C, Sun L, Assad-Garcia N, Richter RA, Smith HO, et al. Polar Effects of Transposon Insertion into a Minimal Bacterial Genome. J Bacteriol. 2019;201(19). Epub 20190906. doi: 10.1128/JB.00185-19. PubMed PMID: 31262838; PubMed Central PMCID: PMCPMC6755753.
61. Lam MMC, Wick RR, Judd LM, Holt KE, Wyres KL. Kaptive 2.0: updated capsule and lipopolysaccharide locus typing for the Klebsiella pneumoniae species complex. Microb Genom. 2022;8(3). doi: 10.1099/mgen.0.000800. PubMed PMID: 35311639; PubMed Central PMCID: PMCPMC9176290.
62. Pain A, Ott A, Amine H, Rochat T, Bouloc P, Gautheret D. An assessment of bacterial small RNA target prediction programs. RNA Biol. 2015;12(5):509-13. doi: 10.1080/15476286.2015.1020269. PubMed PMID: 25760244; PubMed Central PMCID: PMCPMC4615726.
63. Waters LS, Storz G. Regulatory RNAs in bacteria. Cell. 2009;136(4):615-28. doi: 10.1016/j.cell.2009.01.043. PubMed PMID: 19239884; PubMed Central PMCID: PMCPMC3132550.
64. Jana B, Cain AK, Doerrler WT, Boinett CJ, Fookes MC, Parkhill J, et al. The secondary resistome of multidrug-resistant Klebsiella pneumoniae. Sci Rep. 2017;7:42483. Epub 20170215. doi: 10.1038/srep42483. PubMed PMID: 28198411; PubMed Central PMCID: PMCPMC5309761.
65. Dorman MJ, Feltwell T, Goulding DA, Parkhill J, Short FL. The Capsule Regulatory Network of Klebsiella pneumoniae Defined by density-TraDISort. mBio. 2018;9(6). Epub 20181120. doi: 10.1128/mBio.01863-18. PubMed PMID: 30459193; PubMed Central PMCID: PMCPMC6247091.
66. Jung HJ, Littmann ER, Seok R, Leiner IM, Taur Y, Peled J, et al. Genome-Wide Screening for Enteric Colonization Factors in Carbapenem-Resistant ST258 Klebsiella pneumoniae. mBio. 2019;10(2). Epub 20190312. doi: 10.1128/mBio.02663-18. PubMed PMID: 30862751; PubMed Central PMCID: PMCPMC6414703.
67. Paczosa MK, Silver RJ, McCabe AL, Tai AK, McLeish CH, Lazinski DW, et al. Transposon Mutagenesis Screen of Klebsiella pneumoniae Identifies Multiple Genes Important for Resisting Antimicrobial Activities of Neutrophils in Mice. Infect Immun. 2020;88(4). Epub 20200323. doi: 10.1128/IAI.00034-20. PubMed PMID: 31988174; PubMed Central PMCID: PMCPMC7093148.
68. Ma P, He LL, Pironti A, Laibinis HH, Ernst CM, Manson AL, et al. Genetic determinants facilitating the evolution of resistance to carbapenem antibiotics. Elife. 2021;10. Epub 20210419. doi: 10.7554/eLife.67310. PubMed PMID: 33871353; PubMed Central PMCID: PMCPMC8079144.
69. Bruchmann S, Feltwell T, Parkhill J, Short FL. Identifying virulence determinants of multidrug-resistant Klebsiella pneumoniae in Galleria mellonella. Pathog Dis. 2021;79(3). doi: 10.1093/femspd/ftab009. PubMed PMID: 33512418; PubMed Central PMCID: PMCPMC7981267.
70. Chao MC, Abel S, Davis BM, Waldor MK. The design and analysis of transposon insertion sequencing experiments. Nat Rev Microbiol. 2016;14(2):119-28. doi: 10.1038/nrmicro.2015.7. PubMed PMID: 26775926; PubMed Central PMCID: PMCPMC5099075.
71. Lampe DJ, Churchill ME, Robertson HM. A purified mariner transposase is sufficient to mediate transposition in vitro. EMBO J. 1996;15(19):5470-9. PubMed PMID: 8895590; PubMed Central PMCID: PMCPMC452289.
72. Mas G, Thoma J, Hiller S. The Periplasmic Chaperones Skp and SurA. Subcell Biochem. 2019;92:169-86. doi: 10.1007/978-3-030-18768-2_6. PubMed PMID: 31214987.

73. Caza M, Kronstad JW. Shared and distinct mechanisms of iron acquisition by bacterial and fungal pathogens of humans. Front Cell Infect Microbiol. 2013;3:80. Epub 20131119. doi: 10.3389/fcimb.2013.00080. PubMed PMID: 24312900; PubMed Central PMCID: PMCPMC3832793.
74. Iwadate Y, Ramezanifard R, Golubeva YA, Fenlon LA, Slauch JM. PaeA (YtfL) protects from cadaverine and putrescine stress in Salmonella Typhimurium and E. coli. Mol Microbiol. 2021;115(6):1379-94. Epub 20210203. doi: 10.1111/mmi.14686. PubMed PMID: 33481283.
75. Xu Y, Liang Z, Legrain C, Ruger HJ, Glansdorff N. Evolution of arginine biosynthesis in the bacterial domain: novel gene-enzyme relationships from psychrophilic Moritella strains (Vibrionaceae) and evolutionary significance of N-alpha-acetyl ornithinase. J Bacteriol. 2000;182(6):1609-15. doi: 10.1128/JB.182.6.1609-1615.2000. PubMed PMID: 10692366; PubMed Central PMCID: PMCPMC94458.
76. Chambers ST, Lever M. Betaines and urinary tract infections. Nephron. 1996;74(1):1-10. doi: 10.1159/000189274. PubMed PMID: 8883013.
77. Chaturvedi KS, Hung CS, Crowley JR, Stapleton AE, Henderson JP. The siderophore yersiniabactin binds copper to protect pathogens during infection. Nat Chem Biol. 2012;8(8):731-6. Epub 20120708. doi: 10.1038/nchembio.1020. PubMed PMID: 22772152; PubMed Central PMCID: PMCPMC3600419.
78. Cassat JE, Skaar EP. Iron in infection and immunity. Cell Host Microbe. 2013;13(5):509-19. doi: 10.1016/j.chom.2013.04.010. PubMed PMID: 23684303; PubMed Central PMCID: PMCPMC3676888.
79. Banerjee R, Weisenhorn E, Schwartz KJ, Myers KS, Glasner JD, Perna NT, et al. Tailoring a Global Iron Regulon to a Uropathogen. mBio. 2020;11(2). Epub 20200324. doi: 10.1128/mBio.00351-20. PubMed PMID: 32209682; PubMed Central PMCID: PMCPMC7157518.
80. Huang SH, Wang CK, Peng HL, Wu CC, Chen YT, Hong YM, et al. Role of the small RNA RyhB in the Fur regulon in mediating the capsular polysaccharide biosynthesis and iron acquisition systems in Klebsiella pneumoniae. BMC Microbiol. 2012;12(1):148. Epub 20120724. doi: 10.1186/1471-2180-12-148. PubMed PMID: 22827802; PubMed Central PMCID: PMCPMC3423075.
81. Troxell B, Hassan HM. Transcriptional regulation by Ferric Uptake Regulator (Fur) in pathogenic bacteria. Front Cell Infect Microbiol. 2013;3:59. Epub 20131002. doi: 10.3389/fcimb.2013.00059. PubMed PMID: 24106689; PubMed Central PMCID: PMCPMC3788343.
82. Seo SW, Kim D, Latif H, O'Brien EJ, Szubin R, Palsson BO. Deciphering Fur transcriptional regulatory network highlights its complex role beyond iron metabolism in Escherichia coli. Nat Commun. 2014;5(1):4910. Epub 20140915. doi: 10.1038/ncomms5910. PubMed PMID: 25222563; PubMed Central PMCID: PMCPMC4167408.
83. Doorduijn DJ, Heesterbeek DAC, Ruyken M, de Haas CJC, Stapels DAC, Aerts PC, et al. Polymerization of C9 enhances bacterial cell envelope damage and killing by membrane attack complex pores. PLOS Pathogens. 2021;17(11):e1010051. doi: 10.1371/journal.ppat.1010051.
84. Onsare RS, Micoli F, Lanzilao L, Alfini R, Okoro CK, Muigai AW, et al. Relationship between antibody susceptibility and lipopolysaccharide O-antigen characteristics of invasive and gastrointestinal nontyphoidal Salmonellae isolates from Kenya. PLoS Negl Trop Dis. 2015;9(3):e0003573. Epub 20150304. doi: 10.1371/journal.pntd.0003573. PubMed PMID: 25739091; PubMed Central PMCID: PMCPMC4352093.

85. Salamon H, Nissim-Eliraz E, Ardronai O, Nissan I, Shpigel NY. The role of O-polysaccharide chain and complement resistance of Escherichia coli in mammary virulence. Vet Res. 2020;51(1):77. Epub 20200615. doi: 10.1186/s13567-020-00804-x. PubMed PMID: 32539761; PubMed Central PMCID: PMCPMC7294653.
86. Rai AK, Mitchell AM. Enterobacterial Common Antigen: Synthesis and Function of an Enigmatic Molecule. mBio. 2020;11(4). Epub 20200811. doi: 10.1128/mBio.01914-20. PubMed PMID: 32788387; PubMed Central PMCID: PMCPMC7439462.
87. Frirdich E, Whitfield C. Characterization of Gla(KP), a UDP-galacturonic acid C4-epimerase from Klebsiella pneumoniae with extended substrate specificity. J Bacteriol. 2005;187(12):4104-15. doi: 10.1128/JB.187.12.4104-4115.2005. PubMed PMID: 15937173; PubMed Central PMCID: PMCPMC1151718.
88. Ramos PI, Picao RC, Vespero EC, Pelisson M, Zuleta LF, Almeida LG, et al. Pyrosequencing-based analysis reveals a novel capsular gene cluster in a KPC-producing Klebsiella pneumoniae clinical isolate identified in Brazil. BMC Microbiol. 2012;12(1):173. Epub 20120811. doi: 10.1186/1471-2180-12-173. PubMed PMID: 22882772; PubMed Central PMCID: PMCPMC3438125.
89. Yeow J, Tan KW, Holdbrook DA, Chong ZS, Marzinek JK, Bond PJ, et al. The architecture of the OmpC-MlaA complex sheds light on the maintenance of outer membrane lipid asymmetry in Escherichia coli. J Biol Chem. 2018;293(29):11325-40. Epub 20180530. doi: 10.1074/jbc.RA118.002441. PubMed PMID: 29848551; PubMed Central PMCID: PMCPMC6065193.
90. Tan BK, Bogdanov M, Zhao J, Dowhan W, Raetz CR, Guan Z. Discovery of a cardiolipin synthase utilizing phosphatidylethanolamine and phosphatidylglycerol as substrates. Proc Natl Acad Sci U S A. 2012;109(41):16504-9. Epub 20120917. doi: 10.1073/pnas.1212797109. PubMed PMID: 22988102; PubMed Central PMCID: PMCPMC3478633.
91. Rigel NW, Schwalm J, Ricci DP, Silhavy TJ. BamE modulates the Escherichia coli beta-barrel assembly machine component BamA. J Bacteriol. 2012;194(5):1002-8. Epub 20111216. doi: 10.1128/JB.06426-11. PubMed PMID: 22178970; PubMed Central PMCID: PMCPMC3294770.
92. Nguyen D, Kelly K, Qiu N, Misra R. YejM Controls LpxC Levels by Regulating Protease Activity of the FtsH/YciM Complex of Escherichia coli. J Bacteriol. 2020;202(18). Epub 20200825. doi: 10.1128/JB.00303-20. PubMed PMID: 32540932; PubMed Central PMCID: PMCPMC7925073.
93. Hsieh PF, Wu MC, Yang FL, Chen CT, Lou TC, Chen YY, et al. D-galactan II is an immunodominant antigen in O1 lipopolysaccharide and affects virulence in Klebsiella pneumoniae: implication in vaccine design. Front Microbiol. 2014;5:608. Epub 20141119. doi: 10.3389/fmicb.2014.00608. PubMed PMID: 25477867; PubMed Central PMCID: PMCPMC4237132.
94. Ares MA, Fernández-Vázquez JL, Rosales-Reyes R, Jarillo-Quijada MD, von Bargen K, Torres J, et al. H-NS Nucleoid Protein Controls Virulence Features of Klebsiella pneumoniae by Regulating the Expression of Type 3 Pili and the Capsule Polysaccharide. Front Cell Infect Microbiol. 2016;6:13. Epub 20160209. doi: 10.3389/fcimb.2016.00013. PubMed PMID: 26904512; PubMed Central PMCID: PMCPMC4746245.
95. Sledjeski D, Gottesman S. A small RNA acts as an antisilencer of the H-NS-silenced rcsA gene of Escherichia coli. Proc Natl Acad Sci U S A. 1995;92(6):2003-7. doi: 10.1073/pnas.92.6.2003. PubMed PMID: 7534408; PubMed Central PMCID: PMCPMC42411.
96. Ebel W, Trempy JE. Escherichia coli RcsA, a positive activator of colanic acid capsular polysaccharide synthesis, functions To activate its own expression. J Bacteriol.

1999;181(2):577-84. doi: 10.1128/jb.181.2.577-584.1999. PubMed PMID: 9882673; PubMed Central PMCID: PMCPMC93413.
97. Meng J, Young G, Chen J. The Rcs System in Enterobacteriaceae: Envelope Stress Responses and Virulence Regulation. Frontiers in Microbiology. 2021;12. doi: 10.3389/fmicb.2021.627104.
98. Follador R, Heinz E, Wyres KL, Ellington MJ, Kowarik M, Holt KE, et al. The diversity of Klebsiella pneumoniae surface polysaccharides. Microbial Genomics. 2016;2(8). doi: https://doi.org/10.1099/mgen.0.000073.
99. Butaite E, Baumgartner M, Wyder S, Kummerli R. Siderophore cheating and cheating resistance shape competition for iron in soil and freshwater Pseudomonas communities. Nat Commun. 2017;8(1):414. Epub 20170904. doi: 10.1038/s41467-017-00509-4. PubMed PMID: 28871205; PubMed Central PMCID: PMCPMC5583256.
100. Holden VI, Bachman MA. Diverging roles of bacterial siderophores during infection. Metallomics. 2015;7(6):986-95. doi: 10.1039/c4mt00333k. PubMed PMID: 25745886.
101. Clarke BR, Whitfield C. Molecular cloning of the rfb region of Klebsiella pneumoniae serotype O1:K20: the rfb gene cluster is responsible for synthesis of the D-galactan I O polysaccharide. J Bacteriol. 1992;174(14):4614-21. doi: 10.1128/jb.174.14.4614-4621.1992. PubMed PMID: 1378055; PubMed Central PMCID: PMCPMC206256.
102. Touati D. Cloning and mapping of the manganese superoxide dismutase gene (sodA) of Escherichia coli K-12. J Bacteriol. 1983;155(3):1078-87. doi: 10.1128/jb.155.3.1078-1087.1983. PubMed PMID: 6309739; PubMed Central PMCID: PMCPMC217801.
103. Doukyu N, Taguchi K. Involvement of catalase and superoxide dismutase in hydrophobic organic solvent tolerance of Escherichia coli. AMB Express. 2021;11(1):97. Epub 20210629. doi: 10.1186/s13568-021-01258-w. PubMed PMID: 34189628; PubMed Central PMCID: PMCPMC8241964.
104. Najmuldeen H, Alghamdi R, Alghofaili F, Yesilkaya H. Functional assessment of microbial superoxide dismutase isozymes suggests a differential role for each isozyme. Free Radic Biol Med. 2019;134:215-28. Epub 20190115. doi: 10.1016/j.freeradbiomed.2019.01.018. PubMed PMID: 30658083.
105. Flores-Mireles AL, Walker JN, Caparon M, Hultgren SJ. Urinary tract infections: epidemiology, mechanisms of infection and treatment options. Nat Rev Microbiol. 2015;13(5):269-84. Epub 20150408. doi: 10.1038/nrmicro3432. PubMed PMID: 25853778; PubMed Central PMCID: PMCPMC4457377.
106. Murdoch CC, Skaar EP. Nutritional immunity: the battle for nutrient metals at the host-pathogen interface. Nat Rev Microbiol. 2022;20(11):657-70. Epub 20220531. doi: 10.1038/s41579-022-00745-6. PubMed PMID: 35641670; PubMed Central PMCID: PMCPMC9153222.
107. Eberly AR, Floyd KA, Beebout CJ, Colling SJ, Fitzgerald MJ, Stratton CW, et al. Biofilm Formation by Uropathogenic Escherichia coli Is Favored under Oxygen Conditions That Mimic the Bladder Environment. Int J Mol Sci. 2017;18(10). Epub 20170930. doi: 10.3390/ijms18102077. PubMed PMID: 28973965; PubMed Central PMCID: PMCPMC5666759.
108. Cornelis P, Wei Q, Andrews SC, Vinckx T. Iron homeostasis and management of oxidative stress response in bacteria. Metallomics. 2011;3(6):540-9. Epub 20110513. doi: 10.1039/c1mt00022e. PubMed PMID: 21566833.
109. Adler C, Corbalan NS, Peralta DR, Pomares MF, de Cristobal RE, Vincent PA. The alternative role of enterobactin as an oxidative stress protector allows Escherichia coli colony development. PLoS One. 2014;9(1):e84734. Epub 20140102. doi:

10.1371/journal.pone.0084734. PubMed PMID: 24392154; PubMed Central PMCID: PMCPMC3879343.

110. Peralta DR, Adler C, Corbalan NS, Paz Garcia EC, Pomares MF, Vincent PA. Enterobactin as Part of the Oxidative Stress Response Repertoire. PLoS One. 2016;11(6):e0157799. Epub 20160616. doi: 10.1371/journal.pone.0157799. PubMed PMID: 27310257; PubMed Central PMCID: PMCPMC4911079.

111. Guest RL, Court EA, Waldon JL, Schock KA, Raivio TL. Impaired Efflux of the Siderophore Enterobactin Induces Envelope Stress in Escherichia coli. Front Microbiol. 2019;10:2776. Epub 20191206. doi: 10.3389/fmicb.2019.02776. PubMed PMID: 31866967; PubMed Central PMCID: PMCPMC6908949.

112. Singh S, Wilksch JJ, Dunstan RA, Mularski A, Wang N, Hocking D, et al. LPS O Antigen Plays a Key Role in Klebsiella pneumoniae Capsule Retention. Microbiology Spectrum. 2022;10(4):e01517-21. doi: doi:10.1128/spectrum.01517-21.